Deposition and separation of W and Mo from aqueous solutions with simultaneous hydrogen production in stacked bioelectrochemical systems (BESs): Impact of heavy metals W(VI)/Mo(VI) molar ratio, initial pH and electrode material

March 21, 2018

Submitted to J Hazard Mater

Deposition and separation of W and Mo from aqueous solutions with simultaneous hydrogen production in stacked bioelectrochemical systems (BESs): Impact of heavy metals W(VI)/Mo(VI) molar ratio, initial pH and electrode material

Liping Huang[1,*], Ming Li[1], Yuzhen Pan[2], Xie Quan[1], Jinhui Yang[2], Gianluca Li Puma[3,*]

1. Key Laboratory of Industrial Ecology and Environmental Engineering, Ministry of Education (MOE), School of Environmental Science and Technology, Dalian University of Technology, Dalian 116024, China

2. College of Chemistry, Dalian University of Technology, Dalian 116024, China

3. Environmental Nanocatalysis & Photoreaction Engineering, Department of Chemical Engineering, Loughborough University, Loughborough LE11 3TU, United Kingdom

Corresponding authors:

(L. Huang) lipinghuang@dlut.edu.cn

(G. Li Puma) g.lipuma@lboro.ac.uk

The authors declare no competing financial interest.

Abstract: The deposition and separation of W and Mo from aqueous solutions with simultaneous hydrogen production was investigated in stacked bioelectrochemical systems (BESs) composed of microbial electrolysis cell (1#) serially connected with parallel connected microbial fuel cell (2#). The impact of W/Mo molar ratio (in the range 0.01 mM : 1 mM and vice-versa), initial pH (1.5 to 4.0) and cathode material (stainless steel mesh (SSM), carbon rod (CR) and titanium sheet (TS)) on the BES performance was systematically investigated. The concentration of Mo(VI) was more influential than W(VI) in determining the rate of deposition of both metals and the rate of hydrogen production. Complete metal recovery was achieved at equimolar W/Mo ratio of 0.05 mM : 0.05 mM. The rates of metal deposition and hydrogen production increased at acidic pH, with the fastest rates at pH 1.5. The morphology of the metal deposits and the valence of the Mo were correlated with W/Mo ratio and pH. CR cathodes (2#) coupled with SSM cathodes (1#) achieved a significant rate of hydrogen production (0.82 ± 0.04 $m^3/m^3/d$) with W and Mo deposition (0.049 ± 0.003 mmol/L/h and 0.140 ± 0.004 mmol/L/h (1#); 0.025 ± 0.001 mmol/L/h and 0.090 ± 0.006 mmol/L/h (2#)).

Keywords: Bioelectrochemical system; microbial fuel cell; microbial electrolysis cells; W and Mo deposition; hydrogen production

1 Introduction

Tungsten (W) and molybdenum (Mo) transition metals are valuable alloying resources used in various products such as electrochromic materials, gas sensors and lithium ion batteries, in addition to be contained in a range of materials such as special steels and catalysts for petrochemical industries [1-2]. The 2011 annual global production of W and Mo has been reported as 73000 t and 264000 t respectively, with over 80% of W and nearly 40% of Mo being produced in China [3-4]. The extraction of W and Mo from natural ores is an energy intensive process, requiring approximately 11600 kWh/ton of products [5]. The ore dressing wastewater produced during the extraction process of the metals contains a large amount of W and Mo ranging from 10 mg/L to 1000 mg/L, in addition to their existence in the leaching liquor of the spent industrial products [3,6]. The environmental and economic sustainability of the mining process, therefore, requires the recovery and separation of W and Mo from the leaching liquor and from industrial wastewater.

Conventional processes that have been proposed for the extraction and recovery of W and Mo from mining ores include solvent extraction, ion exchange, membrane separation, chemical precipitation and electrochemical treatment [3,7-9]. However, significant challenges remain, including the reduction of the energy consumption and the treatment cost, the reduction of the sludge produced during the treatment and the requirement of bringing the concentration levels of W(VI) and Mo(VI) in the wastewater effluents below the required environmental standards.

This study addresses novel bioelectrochemical systems (BESs) which may

provide an alternative and innovative method for the simultaneous recovery and separation of W and Mo from industrial and mining aqueous effluents [10]. BES multifunctional metallurgical processes have been conceived and intensively investigated, in recent years since they provides cost-effective methods for the extraction and separation of metals [11-12]. In BESs organic matter is oxidized in the anodic chamber while dissolved metals may be simultaneously either reduced in the cathodic chamber or oxidized in the anodic chamber, with the potential of producing free energy [11-14]. BESs operate with zero or minimal external energy consumption, generate very little sludge and require minimal reactor maintenance [15-18]. Multiple metals including V(V), Cr(VI), As(III), Tl (I), Cd(II), Mn(II), Co(II), Ni(II) and Cu(II) [11-12,16,19-27] have been recovered in single units of either microbial fuel cell (MFC) or microbial electrolysis cell (MEC). Differently, stacked metallurgical BESs, configured with MFC units providing in-situ the voltage output to drive the operation of electrically connected MECs, exhibited more merits than single MFC or MEC units. Stacked metallurgical BESs have been conceptually explored for the recovering and separation of multiple metals such as, Cr(VI), Cu(II) and Cd(II), Cu(II) and Co(II), and Cu(II), Co(II) and Li(I) [28-32]. The concept of using optimized MFC and MEC stacked BESs for the efficient deposition and separation of W(VI) and Mo(VI) from mixed aqueous solutions with simultaneous hydrogen production has been demonstrated in our recent study [10] using an initial pH of 2.0, a W(VI)/Mo(VI) molar ratio of 1 : 1 and a stainless steel sheet cathode electrode. However, the impact of the operating parameters require further investigation, in order to optimize the

deposition, separation and recovery of W and Mo metals from practical wastes and wastewaters, with simultaneous hydrogen production.

The concentrations of W(VI) and Mo(VI) in the ores and leaching liquor of spent catalysts are dependent on the characteristics of the mining site or industrial process, with some cases presenting an excess of Mo(VI) and lower amount of W(VI) or vice-versa [4-6,9]. The concentrations of W(VI) and Mo(VI) in the ore dressing wastewater produced during the extraction process, are also closely correlated with the extraction process used. Thus, significant fluctuations in the concentrations of W(VI) and Mo(VI) in the wastewater generally occurs [3,5-6], which translates in variable rates of W and Mo deposition, and thus variable rates of hydrogen production in the MEC units of the stacked BESs. Similarly, pH plays a significant role on the nature of the W and Mo ionic forms present in aqueous solution, on the degree of polymerization of W in electrochemical processes [33], and on the rate of hydrogen evolution in MECs [34-35]. Furthermore, the cathode material also plays an important role. A range of cathodes materials including carbon rod, carbon plate, stainless steel mesh and titanium sheet have been proposed for the recovery of Co(II), Cu(II) and/or Cd(II) in single MFC or MEC units and even stacked BESs [29-31,36-39]. However, the performance of only a few of them has been compared under the same operational conditions [30]. The materials used to recover W and Mo in conventional electrochemical processes operated under galvanic mode include titanium, platinum, nickel, copper and gold [2,40-41]. In particular, W and Mo deposits on these materials also may act as catalysts for the evolution of hydrogen [40-42]. Therefore, the

reduction of heavy metals and the reduction of protons to hydrogen may be competing processes for the cathodic electrons, particularly at low metal concentrations [37-38,43]. Such occurrence may call for the use of different cathodic material and/or experimental conditions depending on the desired treatment objectives.

In this study, stacked BESs were constructed to investigate the impact of the W(VI)/Mo(VI) molar ratio (herein reported as W/Mo for brevity), the initial pH and the cathode electrode material on the rates of W and Mo deposition from aqueous solutions, and on the simultaneous rates of hydrogen production. The W and Mo molar ratio was varied in the range of 0.01 : 1 and vice-versa. The initial pH in the cathodic chamber containing the mixed metals ranged from 1.5 to 4.0, and stainless steel mesh (SSM), carbon rod (CR) and titanium sheet (TS) were systematically explored as cathode materials. The BESs system performance was elucidated by linear sweep voltammetry (LSV), scanning electronic microscopy (SEM), X-ray photoelectron spectroscopy (XPS) and electrochemical impedance spectroscopy (EIS). Cathode potential, current and voltage output from the MFC units applied to the MECs (applied voltage) were employed to assess the rate of W and Mo deposition, the metals separation factor and the rate of hydrogen production. The concept of complete metal recovery was also investigated.

2 Materials and Methods

2.1 BESs assembly

Stacked BESs were designed with one MFC (1#) serially connected with three parallel MFCs (2#) (Fig. S1) as a result of previous optimization of the modules with

multiple units [10]. Each reactor unit was made of two-chambers (14 ml operating volume) separated by a cation exchange membrane (CMI-7000 Membranes International, Glen Rock, NJ). Porous graphite felts (1.0 × 1.0 × 1.0 cm, San Ye Co., Beijing, China) were used as anodes [44], whereas SSS (2.0 × 2.0 cm, Qing Yuan Co., China) were used as the cathodes of both the 1# and the 2# units. A glass tube with an inner diameter of 8 mm was glued to the top of the 1# unit to create a total headspace of 12 mL for hydrogen collection [10,44]. A reference electrode (Ag/AgCl, 195 mV vs. SHE) was installed in the cathodic chamber to measure the electrode potential, with all potentials reported vs. SHE. The reactors were wrapped with aluminum foil to ensure darkness, to avoid the algae growth on the anodes and possible side reactions on the cathodes. The properties of the 2# units have been reported as average values for the sake of clarity, since the differences among the three units connected in parallel were insignificant.

2.2 Inoculation and operation

Anodic inoculation was exactly the same as previously described [28-30]. Mixed W(VI) and Mo(VI) aqueous solutions were prepared using $Na_2WO_4 \cdot 2H_2O$ and $Na_2MoO_4 \cdot 2H_2O$ (Kaida Chemical Co. Ltd., Tianjin, China). The W and Mo molar ratio (mM : mM) in the cathodic chamber was varied as 1 : 1, 0.1 : 1, 0.05 : 1, 0.01 : 1, 1 : 0.1, 1 : 0.05, and 1 : 0.01, and the initial pH was 1.5, 2.0, 2.5, 3.0, 3.5 and 4.0. Also experiments were conducted at equimolar concentrations of 0.1 : 0.1 and 0.05 : 0.05. Solution conductivity was invariably regulated to the maximal 6.60 mS/cm associated with the most acidic pH of 1.5, to exclude the effect of solution

conductivity on system performance [45]. SSM, CR (Chijiu Duratight Carbon Co., Qingdao, China) or TS (Qingyuan Co., China) cathodes (1#) were coupled with SSM or CR cathodes (2#) with equal geometric areas (2.0 × 2.0 cm). The stacked BESs were operated in fed-batch mode at room temperature (25 ± 3 ºC). Three duplicate BESs were used in all experiments.

Control experiments with single W(VI) or Mo(VI) metal in solution were performed to reflect the impact of the binary-component on the system performance. Control experiments under open circuit conditions (OCCs) reflected the effect of current on W and Mo deposition. Other control experiments using the 1# or the 2# units only were performed to illustrate the roles played by each unit on system performance.

2.3 Measurements and analyses

The W(VI) and Mo(VI) concentrations in the catholyte were measured using standard methods [46]. The electrical data were monitored with an automatic data acquisition system (PISO-813, Hongge Co.,Taiwan). The electrical current was calculated from the voltage read across a small external resistance (10 Ω). The hydrogen in the headspace of the cathodic chambers was sampled and analyzed as previously described [10,37-38,44].

The rates of W (R_W, mmol/L/h) and Mo (R_{Mo}, mmol/L/h) deposition on the cathodes was calculated from Eqs. S1 – 2, whereas the power density was normalized to the projected surface area of the separator [10]. The rate of hydrogen production and the separation factor ε were calculated from Eqs. S3 and S4, respectively [10,36].

LSVs were conducted using a potentiostat (CHI 770c, Chenhua, Shanghai) at a scan rate of 1.0 mV/s. The inner resistance of the BES units at different initial pH and W/Mo molar ratios was quantified by EIS (Bio-Logic VMP3) as previously described [10,39,43,47]. The morphologies and valences of the products on the cathode were observed by SEM (Hitachi S-4800) and determined by XPS (Kratos AXIS Ultra DLD). One-way ANOVA in SPSS 19.0 was used to analyze the differences among the data, and all of the data indicated significance levels of $p < 0.05$.

3 Results and discussion

3.1 The impact of W/ Mo molar ratio

At a fixed Mo concentration of 1.0 mM, higher W concentrations favored the deposition of W (Fig. 1A) and negligibly affected the deposition of Mo (Fig. 1B) in both the 1# and the 2# units. The rate of deposition of W was 0.079 ± 0.003 mmol/L/h (1#) and 0.050 ± 0.001 mmol/L/h (2#) (Fig. 1A), while for Mo it was 0.193 ± 0.002 mmol/L/h (1#) and 0.138 ± 0.001 mmol/L/h (2#) (Fig. 1B), at the higher concentration of W investigated (1.0 mM). Greater amounts of W and Mo were invariably deposited in the 1# unit, rather than in the 2# units (Fig. 1A and B), which was ascribed to the voltage output from the 2# units and applied to the 1# unit (Fig. 1C) for the consequent higher currents (Fig. 1D) and more negative cathode potentials (Fig. 1E) in the 1# unit. Higher current and more negative potentials favor the rate of deposition of oxidative metals on the cathodes of BESs [11-12]. The observed polarization curves and electrode potentials as a function of the current (Fig. S2) further demonstrated the significance and impact of the W concentration on the BESs

performance. The similar values of applied voltages, in the range 0.10 – 0.11 V (Fig. 1C), led to the simultaneous evolution of hydrogen at variable rates (0.34 – 0.41 m^3/m^3 d) in the 1# unit, during the deposition of the metals (Fig. 1F). This result also reflected an insignificant effect of W concentrations on the rate of hydrogen production in the 1# unit.

Here Fig. 1

At a fixed W concentration of 1.0 mM, a decrease in Mo concentration decreased the rate of deposition of W (Fig. 2A) and Mo (Fig. 2B) in both the 1# and the 2# units with varying degrees. This resulted in high values of the separation factors equal to 717 ± 4 (1#) and 200 ± 8 (2#), at a W/Mo molar ratio of 1 : 0.1 (Table 1), which were significantly higher than the values (80 to 105) reported in conventional solvent extraction processes [8]. Lower Mo concentrations led to decreased currents (Fig. 2C) and less negative cathode potentials (Fig. 2D) in the 1# unit. It also significantly decreased the applied voltages (Fig. 2E), consistent with the polarization curves and the cathodic potentials as a function of current (Fig. S3), all of which explained the decreased rate of hydrogen production observed (Fig. 2F).

Collectively, the results in Fig. 1 and Fig. 2 show that Mo(VI) was more influential than W(VI) in determining an increase in the rate of deposition of both metals and in the rate of hydrogen production. The influential role of Mo(VI) for either W(VI) recovery or as catalysts for hydrogen evolution in conventional chemical/electrochemical processes has been also shown in other studies [2,7-8,41,48]. Binary mixtures of W(VI) and Mo(VI) reportedly forms diverse molybdotungstates

species, which favor the further deposition of W(VI), however, the deposition of W is inhibited in the absence of Mo(VI) in conventional chemical/electrochemical processes [7,49]. Thus, at high W/Mo molar ratios, the rates of deposition of the metals and hydrogen production were diminished in the stacked BESs.

Here Fig. 2

Here Table 1

The W/Mo molar ratio also influenced the morphology of the metals deposited over the stacked BESs cathodes. Smaller and more homogeneous particles were observed on the cathodes of both the 1# (Fig. S4A) and the 2# (Fig. S4B) units at a W/Mo molar ratio of 1 : 0.01, in comparison to those at a W/Mo ratio of 1 : 1 (Fig. S4C and D). Conversely, a W/Mo molar ratio of 0.01 : 1 led to the presence of irregular deposits in the 1# unit (Fig. S4E) complemented by dense layer deposits in the 2# units (Fig. S4F).

The XPS spectra for the W4f or Mo3d core electronic transitions exhibited the characteristic $4f_{7/2}$ and $4f_{5/2}$ or $3d_{5/2}$ and $3d_{3/2}$ doublet of peaks at 35.8 and 37.9 eV assigned to W(VI) in WO_3 [50], whereas the peaks at 232.9 and 236.0, 231.4 and 234.5, and 230.0 and 233.1 eV corresponded to $Mo3d_{5/2}$ and $Mo3d_{3/2}$ in MoO_3, Mo_2O_5 and MoO_2, respectively (Table S1) [42]. Similar peaks at 35.9 and 38.1 eV were observed in both the 1# (Fig. 3A and E) and the 2# (Fig. 3C and G) units regardless of the W/Mo molar ratio (i.e., high (1 : 0.01) (Fig. 3A and C) or low (0.01 : 1) (Fig. 3E and G)). The catholyte at the end of each fed-batch cycle operation instantly changed in color in the absence of N_2 protection, consistent with the report

that W(V) as a reduced product is highly unstable and easily oxidized to W(VI) due to the sampling procedures [2]. Thus, these similar peaks (Fig. 3A, 3C, 3E and 3G) could presumably be the result from the re-oxidation of the W reduced products. In contrast, the valence of the Mo deposits was strongly correlated with the W/Mo molar ratio and varied among the different units (Fig. 3B, D, F and H). Stronger Mo(V) and Mo(IV) signals were observed at a low W/Mo molar ratio of 0.01 : 1 in the 1# unit (Fig. 3F) rather than in the 2# units (Fig. 3H and Table S1), while much weaker signals were observed at a W/Mo molar ratio of 1 : 0.01 in the 1# unit (Fig. 3B and Table S1). This result demonstrates that Mo(VI) was more easily reduced to Mo(V) rather than Mo(IV).

Here Fig. 3

The variation of the cathode resistances at different W/Mo molar ratios was determined by EIS (Fig. 4) through the fitting of the observed spectra to equivalent electrical circuits (Fig. S5 and Table S2). The ohmic resistance (R_o) at low W/Mo ratios of 0.05 : 1 and 0.01 : 1 was equivalent to that at equimolar W/Mo ratio of 1 : 1, but the polarization resistance (R_p) was higher and the diffusional resistance (R_d) was lower (Fig. 4A and Table S2). Therefore, the deposition of Mo increased the activation loss and decreased the diffusional loss. High W/Mo ratios instead, invariably increased the resistances R_o, R_p and R_d (Fig. 4B and Table S2), consistent with the polarization curves and cathode potentials as a function of current (Fig. S3), implying that the W deposits had a stronger effect than Mo on the resistances. In the control experiments performed with either W(VI) or Mo(VI) in solution, the resistances R_o, R_p and R_d were appreciably higher than those observed with the binary metals (Fig.

4C and Table S2).

Here Fig. 4

3.2 Effect of initial pH

The initial pH of the catholyte was varied in the range from 1.5 to 4.0. At acidic pH of 1.5 and 2.0 the highest rates of W and Mo deposition were observed, equaling 0.0785 ± 0.003 – 0.0808 ± 0.004 mmol/L/h (W) and 0.190 ± 0.004 – 0.193 ± 0.002 mmol/L/h (Mo) in the 1# unit, and 0.0501 ± 0.001 – 0.0548 ± 0.001 mmol/L/h (W) and 0.138 ± 0.001 – 0.144 ± 0.005 mmol/L/h (Mo) in the 2# units (Fig. 5A and B). Higher amounts of metals deposited in the 1# than in the 2# units, were generally accompanied by higher separation factors in the former (Table 1), consistent with the higher currents (Fig. 5C) and the more negative cathode potentials (Fig. 5D) observed in the 1# unit, both of which generally favor the reduction of oxidative substrates [11,51]. A decreasing trend of the rate of metal deposition was observed at an initial pH higher than 2.0.

Smaller polarization loss (Fig. S6), higher applied voltage (Fig. 5E) and an appreciable higher rate of hydrogen production (Fig. 5F) were observed at more acidic initial pH in the 1# unit, consistent with the decrease of the pH in the effluents from 5.93 ± 0.08 at an initial pH of 4.0 to 2.27 ± 0.06 at pH 1.5. Other studies, performed with MECs in the absence of W or/and Mo also reported faster rates of hydrogen production at more acidic pH [34-35]. Considering the similar rates of W and Mo depositions at pH 1.5 and 2.0 (Fig. 5A and B), the significantly higher hydrogen production at pH 1.5 implied that hydrogen evolution outcompeted the

deposition of the metals for the available cathodic electrons, alike the electron competition between reductive dechlorination and denitrification [52].

An experiment with pH controlled at 1.5 during the entire operational period was purposely investigated to determine its effect on the metal deposition. An appreciable higher rate of hydrogen production of 2.14 ± 0.07 $m^3/m^3/d$, and enhanced W and Mo deposition rates (W: 0.0965 ± 0.005 mmol/L/h; Mo: 0.227 ± 0.005 mmol/L/h) in the 1# unit were observed, compared to the results obtained without pH control (1.21 ± 0.03 $m^3/m^3/d$, 0.081 ± 0.004 mmol/L/h (W) and 0.190 ± 0.004 mmol/L/h (Mo)). In concert, the results observed supported a significant dependence of the rate of W and Mo deposition with simultaneous hydrogen production on the pH in the catholyte.

Here Fig. 5

The morphology of the W and Mo deposits was significantly influenced by the initial pH in the catholyte. Wider cracks and larger areas surrounded by the cracks in both the 1# and the 2# units (Fig. S7A and B) were observed at pH 1.5, in comparison to the results at pH 2.0 and 4.0, consistent with the morphology of Mn, Mo and W co-deposits in conventional electrochemical processes [33]. Larger W and Mo grain sizes were consistently observed in the 1# (Fig. S7A, C and E) than in the 2# units (Fig. S7B, D and F), and the grain size was inversely correlated with the increase in the initial pH in the same units. The higher currents observed in the 1# than in the 2# units at the same pH (Fig. 5C) resulted in wider cracks and smaller grains, consistent with the tungsten morphology influenced by current in conventional electrochemical processes [53].

The XPS binding energies (Fig. 6) for Mo and W deposits as well as the corresponding area percent (Table S1) showed that at an initial pH 1.5 appreciable higher Mo(IV) products were achieved in the 1# unit (48%, Fig. 6B and Table S2) than in the 2 units (26%, Fig. 6F and Table S2), both of which were higher than the results at an initial pH of 4.0 (13% in 1#, Fig. 6D and 8% in 2#, Fig. 6H and Table S2). These results clearly demonstrate the dependency of the valences of the Mo deposits on the initial pH. Similarly, the peaks associated with W deposits in the 1# unit at pH 1.5 (Fig. 6A) were apparently higher than either in the 2# units at the same pH (Fig. 6E) or in the same 1# unit but at pH 4.0 (Fig. 6C). The lowest peaks were observed in the 2# units at pH 4.0 (Fig. 6G). Collectively, these results demonstrated a significant dependency of the rate of W and Mo deposition, and even the dependence of the valence of the Mo deposits, on the initial pH of the catholyte, and on the units of the stacked BESs.

Here Fig. 6

EIS spectra were used to identify the components of the internal resistances as a function of the initial pH. R_d, R_p and R_o in concert exhibited increase trends with an increase in the initial pH, from 456 Ω, 10.1 Ω and 6.9 Ω at a pH of 1.5, to 11987 Ω, 121.1 Ω and 17.8 Ω at pH 4.0 (Fig. S8 and Table S2). These results clearly illustrated the favorable effect of acidic pH on decreasing the internal resistances of the stacked BESs, consistent with the results shown in Fig. 5.

3.3 Effect of electrode material

The use of inexpensive SSS cathodes in both the 1# and the 2# units achieved the

highest rate of W (Fig. 7A) and Mo deposition (Fig. 7B) with lower rates of hydrogen production (Fig. 7F) and more polarization loss (Fig. S9A and B), in comparison to the other electrodes combinations tested (Fig. 7A, B and F, Fig. S9). SSS cathodes (1#) coupled with the CR cathodes (2#) exhibited similar more negative cathode potentials and higher currents as the configuration using TS (1# unit) and CR (2#) cathodes (Fig. 7C and D), resulting in higher applied voltages (Fig. 7E) and the subsequent significant rate of hydrogen production of 0.82 ± 0.04 $m^3/m^3/d$ (Fig. 7F) with W and Mo deposition (W: 0.049 ± 0.003 mmol/L/h (1#), 0.025 ± 0.001 mmol/L/h (2#); Mo: 0.140 ± 0.004 mmol/L/h (1#), 0.090 ± 0.006 mmol/L/h (2#)) (Fig. 7A and B). Hydrogen evolution is well known to increase the pH in solution [34], which in consequence penalizes the deposition of W and Mo [10], explaining reduced rates of W and Mo deposition at much more negative cathode potentials and higher currents (Fig. 7A – D). The results collectively show that SSS (1#) and CR (2 #) represent well-matched electrodes for efficient W and Mo deposition in the stacked BESs.

Here Fig. 7

3.4 Complete metal recovery

The results reported have shown that the W(VI)/Mo(VI) molar ratio significantly affected the rate of metals deposition, as well as, the rate of hydrogen production in the stacked BESs. W(VI)/Mo(VI) molar ratios smaller or equal to 1 : 1 favoured the deposition of more W and Mo in the 1# than the 2# units with a negligible effect on the rate of hydrogen production (Fig. 1). In contrast, W(VI)/Mo(VI) molar ratios larger than 1 : 1 resulted in similar rates of deposition of both metals in both the 1#

and the 2# units, and more than halved the rate of hydrogen production (Fig. 2). Further experiments with equimolar W(VI)/Mo(VI) molar ratios and lower initial metals concentrations (1 : 1, 0.1 : 0.1 and 0.05 : 0.05) were performed at an initial pH of 2.0 with cathodes of SSS (1#) and CR (2#) to clarify the role of equimolar heavy metals concentration on system performance. The rates of W (Fig. 8A) and Mo (Fig. 8B) deposition decreased when reducing the concentrations of the metals from 1 : 1 to 0.05 : 0.05. At the lower metals concentrations of 0.05 : 0.05, complete heavy metals deposition was achieved in the 1# unit and almost complete deposition (94.3 ± 2.2% (W) and 98.4 ± 0.8% (Mo)) occurred in the 2# units. Simultaneously, lower separation factors (Table 1), smaller currents (Fig. 8C), more positive cathode potentials (Fig. 8D), lower applied voltages (Fig. 8E) and smaller rates of hydrogen production (Fig. 8F) were observed in comparison to the 1 : 1 case. These results demonstrate the feasibility of these stacked BESs for either complete deposition of W and Mo at this lower equivalent W and Mo concentrations, or higher rates of hydrogen production at higher equivalent W and Mo concentrations.

Here Fig. 8

The deposition of binary mixtures of W(VI) and Mo(VI) in stacked BESs have shown synergistic effects on the recovery of the metals and the simultaneous production of hydrogen [10]. However, the optimization of such BESs required further analysis to account for the impact of fluctuations in the concentration of heavy metals and pH in the wastewater [4-6]. Furthermore, the electrode materials exert a significant impact on the rates of other metals deposition and hydrogen production in

BESs [35,37-37,54]. The elucidation of such effects is required for further optimization of BESs, which could ultimately lead to industrial application.

The present study has illustrated the dependency of rates of W and Mo deposition, as well as, hydrogen production on the W/Mo molar ratio, initial pH and electrode material. Mo(VI) was more influential than W(VI) in determining an increase in the rates of deposition of both metals and hydrogen production. The merit of completely depositing W and Mo at an initial equimolar W/Mo ratio of 0.05 : 0.05 gives an advantage of this technology over conventional methods such as ion exchange, chemical precipitation or adsorption [5,9], particularly with low-strength W and Mo wastewaters from either the mining industry processes or wastewater effluents. Such lower concentrations of metals in high strength wastewater could be achieved with the partial recirculation of the effluent back to the influent [55-56] to dilute the feed stream to the stacked BESs to optimal values, achieving enhanced metal deposition and even complete separation of W and Mo (Fig. 1,2 and 8, and Table 1). Practical implementation will also depend on the long-term operation of this system, as well as, the process economics of BESs relative to conventional treatment processes [54]. Although the present economic values of W and Mo deposits are relatively low, the added complexity in the stacked BESs will be paid off with increasing the demand on sustainability and elevated product values due to the depletion of W and Mo resources. The simultaneous production of hydrogen by-product in the MEC units of the stacked BESs further offsets the cost of this technology, although further pilot and full-scale investigations are necessary to

evaluate the long-term operation and stability of the system over feeds with fluctuating physico/chemical properties.

4 Conclusions

Stacked BESs composed of MEC (1#) serially connected with parallel connected MFC (2#) have been shown to be effective in W and Mo deposition and separation with simultaneous hydrogen production. It revealed a dramatic effect of the W/Mo molar ratio, initial pH, and cathode material on the rates observed. The concentration of Mo(VI) was more influential than W(VI) in determining the rate of deposition of both metals and the rate of hydrogen production. Complete metal recovery was achieved at equimolar W/Mo ratio of 0.05 mM : 0.05 mM. Acidic pH favored both the deposition of the metals and the rate of hydrogen production. The BESs comprising CR cathodes (2#) coupled with SSS cathodes (1#) achieved optimal performance. The BESs studied here may provide an alternative and innovative method for the recovery and separation of W and Mo from industrial and mining aqueous effluents with simultaneous hydrogen production.

Acknowledgments

The authors are gratefully acknowledge financial support from the National Natural Science Foundation of China (Nos. 51578104 and 21777017), and the Programme of Introducing Talents of Discipline to Universities (B13012).

References

[1] D. Merki, X. Hu, Recent developments of molybdenum and tungsten sulfides as hydrogen evolution catalysts, Energy Environ. Sci. 4 (2011) 3878-3888, http://dx.doi.org/10.1039/C1EE01970H.

[2] S. Sun, T. Bairachna, E.J. Podlaha, Induced codeposition behavior of electrodeposited NiMoW alloys, J. Electrochem. Soc. 160 (2013) D434-D440, http://dx.doi.org/10.1149/2.014310jes.

[3] T.A. Lasheen, M.E. El-Ahmady, H.B. Hassib, A.S. Helal, Molybdenum metallurgy review: Hydrometallurgical routes to recovery of molybdenum from ores and mineral raw materials, Miner. Process. Extr. Metall. Rev. 36 (2015)145-173, http://dx.doi.org/10.1080/08827508.2013.868347.

[4] T. Ogi, T. Makino, K. Okuyama, W.J. Stark, F. Iskandar, Selective biosorption and recovery of tungsten from an urban mine and feasibility evaluation, Ind. Eng. Chem. Res. 55 (2016) 2903-2910, http://dx.doi.org/10.1021/acs.iecr.5b04843.

[5] Z. Zhao, C. Cao, X. Chen, G. Huo, Separation of macro amounts of tungsten and molybdenum by selective precipitation, Hydrometallurgy 108 (2011) 229-232, https://doi.org/10.1016/j.hydromet.2011.04.006.

[6] R.R. Srivastava, N.K. Mittal, B. Padh, B. Ramachandra Reddy, Removal of tungsten and other impurities from spent HDS catalyst leach liquor by an adsorption route, Hydrometallurgy 127-128 (2012) 77-83, https://doi.org/10.1016/j.hydromet.2012.07.004.

[7] L. Kondrachova, P.H. Benjamin, G. Vijayaraghavan, R.D. Williams, K.J. Stevenson, Cathodic electrodeposition of mixed molybdenum tungsten oxides from peroxo-polymolybdotungstate solutions, Langmuir 22 (2006) 10490-10498, https://doi.org/10.1021/la061299n.

[8] W. Guan, G. Zhang, C. Gao, Solvent extraction separation of molybdenum and tungsten from ammonium solution by H_2O_2-complexation, Hydrometallurgy 127-128 (2012) 84-90, https://doi.org/10.1016/j.hydromet.2012.07.008.

[9] G. Huo, C. Peng, Q. Song, X. Lu, Tungsten removal from molybdate solutions using ion exchange, Hydrometallurgy 147-148 (2014) 217-222, https://doi.org/10.1016/j.hydromet.2014.05.015.

[10] L. Huang, M. Li, Y. Pan, Y. Shi, X. Quan, G. Li Puma, Efficient W and Mo deposition and separation with simultaneous hydrogen production in stacked bioelectrochemical systems, Chem. Eng. J. 327 (2017) 584-596, http://dx.doi.org/10.1016/j.cej.2017.06.149.

[11] H. Wang, Z.J. Ren, Bioelectrochemical metal recovery from wastewater: a review, Water Res. 66 (2014) 219-232, http://dx.doi.org/10.1016/j.waters.2014.08.013.

[12] Y.V. Nancharaiah, S.Venkata Mohan, P.N.L. Lens, Biological and bioelectrochemical recovery of critical and scarce metals, Trends Biotechnol. 34 (2016) 137-155, http://dx.doi.org/10.1016/j.tibtech.2015.11.003.

[13] X. Yong, D. Gu, Y. Wu, Z. Yan, J. Zhou, X. Wu, P. Wei, H. Jia, T. Zheng, Y. Yong, Bio-electron-fenton (BEF) process driven by microbial fuel cells for triphenyltin chloride (TPTC) degradation, J. Hazard. Mater. 324 (2017) 178-183, http://dx.doi.org/10.1016/j.jhazmat.2016.10.047.

[14] Q. Zhao, H. Yu, W. Zhang, F.T. Kabutey, J. Jiang, Y. Zhang, K. Wang, J. Ding, Microbial fuel cell with high content solid wastes as substrates: a review, Front. Environ. Sci. Eng. 11 (2017) 13, http://dx.doi.org/10.1007/s11783-017-0918-6.

[15] O. Modin, X. Wang, X. Wu, S. Rauch, K.K. Fedje,

Bioelectrochemical recovery of Cu, Pb, Cd, and Zn from dilute solutions, J. Hazard. Mater. 235 (2012) 291-297, http://dx.doi.org/10.1016/j.jhazmat.2012.07.058.
[16] M. Peiravi, S.R. Mote, M.K. Mohanty, J. Liu, Bioelectrochemical treatment of acid mine drainage (AMD) from an abandoned coal mine under aerobic condition, J. Hazard. Mater. 333 (2017) 329-338, http://dx.doi.org/10.1016/j.jhazmat.2017.03.045.
[17] O. Modin, F. Aulenta, Three promising applications of microbial electrochemistry for the water sector, Environ. Sci.: Water Res. Technol. 3 (2017) 391-402, http://dx.doi.org/10.1039/C6EW00325G.
[18] M. Wang, Q. Tan, J.F. Chiang, J. Li, Recovery of rare and precious metals from urban mines-A review, Front. Environ. Sci. Eng. 11 (5) (2017) 1, http://dx.doi.org/10.1007/s11783-017-0963-1.
[19] B. Zhang, C. Feng, J. Ni, J. Zhang, W. Huang, Simultaneous reduction of vanadium (V) and chromium (VI) with enhanced energy recovery based on microial fuel cell technology, J. Power Sources 204 (2012) 34-39, http://dx.doi.org/10.1016/j.jpowsour.2012.01.013.
[20] H. Luo, G. Liu, R. Zhang, Y. Bai, S. Fu, Y. Hou, Heavy metal recovery combined with H_2 production from artificial acid mine drainage using the microbial electrolysis cell, J. Hazard. Mater. 270 (2014) 153-159, http://dx.doi.org/10.1016/j.jhazmat.2014.01.050.
[21] N. Colantonio, Y. Kim, Cadmium (II) removal mechanisms in microbial electrolysis cells, J. Hazard. Mater. 311 (2016) 134-141, http://dx.doi.org/10.1016/j.jhazmat.2016.02.062.
[22] Y. Li, B. Zhang, M. Cheng, Y. Li, L. Hao, Spontaneous arsenic (III) oxidation with bioelectricity generation in single-chamber microbial fuel cells, J. Hazard. Mater. 306 (2016) 8-12, http://dx.doi.org/10.1016/j.jhazmat.2015.12.003.
[23] Y. Dong, J.F. Liu, M.R. Sui, Y.P. Qu, J.J. Ambuchi, H.M. Wang, Y.J. Feng, A combined microbial desalination cell and electrodialysis system for copper-containing wastewater treatment and high-salinity-water desalination, J. Hazard. Mater. 321 (2016) 307-315, http://dx.doi.org/10.1016/j.jhazmat.2016.08.034.
[24] D. Wu, L. Huang, X. Quan, G. Li Puma, Electricity generation and bivalent copper reduction as a function of operation time and cathode electrode material in microbial fuel cells, J. Power Sources 307 (2016) 705-714, https://doi.org/10.1016/j.jpowsour.2016.01.022.
[25] R. Qiu, B. Zhang, J. Li, Q. Lv, S. Wang, Q. Gu, Enhanced vanadium (V) reduction and bioelectricity generation in microbial fuel cells with biocathode, J. Power Sources 359 (2017) 379-383, http://dx.doi.org/10.1016/j.jpowsour.2017.05.099.
[26] G. Wang, B. Zhang, S. Li, M. Yang, C. Yin, Simultaneous microbial reduction of vanadium (V) and chromium (VI) by *Shewanella loihica* PV-4, Bioresour. Technol. 227 (2017) 353-358, http://dx.doi.org/10.1016/j.jpowsour.2017.05.099.
[27] Z. Wang, B. Zhang, Y. Jiang, Y. Li, C. He, Spontaneous thallium (I) oxidation with electricity generation in single-chamber microbial fuel cells, Appl. Energy 209

(2018) 33-42, http://dx.doi.org/10.1016/j.apenergy.2017.10.075.
[28] J. Shen, Y. Sun, L. Huang, J. Yang, Microbial electrolysis cells with biocathodes and driven by microbial fuel cells for simultaneous enhanced Co(II) and Cu(II) removal, Front. Environ. Sci. Eng. 9 (2015) 1084-1095, http://dx.doi.org/10.1007/s11783-015-0805-y.
[29] Y. Zhang, L. Yu, D. Wu, L. Huang, P. Zhou, X. Quan, G. Chen, Dependency of simultaneous Cr(VI), Cu(II) and Cd(II) reduction on the cathodes of microbial electrolysis cells self-driven by microbial fuel cells, J. Power Sources 273 (2015) 1103-1113, https://doi.org/10.1016/j.jpowsour.2014.09.126.
[30] D. Wu, Y. Pan, L. Huang, X. Quan, J. Yang, Comparison of Co(II) reduction on three different cathodes of microbial electrolysis cells driven by Cu(II)-reduced microbial fuel cells under various cathode volume conditions, Chem. Eng. J. 266 (2015) 121-132, https://doi.org/10.1016/j.cej.2014.12.078.
[31] D. Wu, Y. Pan, L. Huang, P. Zhou, X. Quan, H. Chen, Complete separation of Cu(II), Co(II) and Li(I) using self-driven MFCs-MECs with stainless steel mesh cathodes under continuous flow conditions, Sep. Purif. Technol. 147 (2015) 114-124, http://dx.doi.org/10.1016/j.seppur.2015.04.016.
[32] M. Li, Y. Pan, L. Huang, Y. Zhang, J. Yang, Continuous flow operation with appropriately adjusting composites in influent for recovery of Cr(VI), Cu(II) and Cd(II) in self-driven MFC-MEC system, Environ. Technol. 38 (2017) 615-628, http://dx.doi.org/10.1080/09593330.2016.1205149.
[33] N.A. Abdel Ghany, S. Meguro, N. Kumagai, K. Asami, K. Hashimoto, Adodically deposited Mn-Mo-Fe oxide anodes for oxygen evolution in hot seawater electrolysis, Mater. Trans. 44 (2003) 2114-2123.
[34] Y. Ruiz, J.A. Baeza, A. Guisasola, Enhanced performance of bioelectrochemical hydrogen production using a pH control strategy, ChemSusChem 8 (2015) 389-397, http://dx.doi.org/10.1002/cssc.201403083.
[35] A. Kadier, M. Sahaid Kalil, P. Abdeshahian, K. Chandrasekhar, A. Mohamed, N. Farhana Azman, W. Logroño, Y. Simayi, A. Abdul Hamid, Recent advances and emerging challenges in microbial electrolysis cells (MECs) for microbial production of hydrogen and value-added chemicals, Renew. Sust. Energ. Rev. 61 (2016) 501-525, https://doi.org/10.1016/j.rser.2016.04.017.
[36] L. Huang, B. Yao, D. Wu, X. Quan, Complete cobalt recovery from lithium cobalt oxide in self-driven microbial fuel cell-microbial electrolysis cell systems, J. Power Sources 259 (2014) 54-64, https://doi.org/10.1016/j.jpowsour.2014.02.061.
[37] Q. Wang, L. Huang, H. Yu, X. Quan, Y. Li, G. Fan, L. Li, Assessment of five different cathode materials for Co(II) reduction with simultaneous hydrogen evolution in microbial electrolysis cells, Inter. J. Hydrogen Energy 40 (2015) 184-196, https://doi.org/10.1016/j.ijhydene.2014.11.014.
[38] Q. Wang, L. Huang, Y. Pan, P. Zhou, X. Quan, B.E. Logan, H. Chen, Cooperative cathode electrode and in situ deposited copper for subsequent enhanced Cd(II) removal and hydrogen evolution in bioelectrochemical systems, Bioresour. Technol. 200 (2016) 565-571, https://doi.org/10.1016/j.biortech.2015.10.084.
[39] Q. Wang, L. Huang, Y. Pan, X. Quan, G. Li Puma, Impact of Fe(III) as an

effective mediator for enhanced Cr(VI) reduction in microbial fuel cells: Reduction of diffusional resistances and cathode overpotentials, J. Hazard. Mater. 321 (2017) 896-906, http://dx.doi.org/10.1016/j.jhazmat.2016.10.011.

[40] N. Tsyntsaru, H. Cesiulis, M. Donten, J. Sort, E. Pellicer, E.J. Podlaha-Murphy, Modern trends in tungsten alloys electrodeposition with iron group metals, Surface Eng. Appl. Electrochem. 48 (2012) 491-520, http://dx.doi.org/10.3103/S1068375512060038.

[41] T.G. Kelly, S.T. Hunt, D.V. Esposito, J.G. Chen, Monolayer palladium supported on molybdenum and tungsten carbide substrates as low-cost hydrogen evolution reaction (HER) electrocatalysts, Inter. J. Hydrogen Energy 38 (2013) 5638-5644, https://doi.org/10.1016/j.ijhydene.2013.02.116.

[42] M. Zhang, D. Lu, G. Yan, J. Wu, J. Yang, Fabrication of Mo+N-codoped TiO_2 nanotube arrays by anodization and sputtering for visible light-induced photoelectrochemical and photocatalytic properties, J. Nanomater. 2013 (2013) 1-9, http://dx.doi.org/10.1155/2013/648346.

[43] Q. Wang, L. Huang, X. Quan, Q. Zhao, Preferable utilization of in-situ produced H_2O_2 rather than externally added for efficient deposition of tungsten and molybdenum in microbial fuel cells, Electrochim. Acta 247C (2017) 880-890, https://doi.org/10.1016/j.electacta.2017.07.079.

[44] Y. Chen, J. Shen, L. Huang, Y. Pan, X. Quan, Enhanced Cd(II) removal with simultaneous hydrogen production in biocathode microbial electrolysis cells in the presence of acetate or $NaHCO_3$, Inter. J. Hydrogen Energy 41 (2016) 13368-13379, https://doi.org/10.1016/j.ijhydene.2016.06.200.

[45] B.E. Logan, Essential data and techniques for conducting microbial fuel cell and other types of bioelectrochemical system experiments, ChemSusChem 5 (2012) 988-994, https://doi.org/10.1002/cssc.201100604.

[46] American Public Health Association, American Water Works Association, Water Pollution Control Federation, Standard methods for the examination of water and wastewater, *20*th edn. American Public Health Association, Washington, 1998.

[47] Z. He, F. Mansfeld, Exploring the use of electrochemical impedance spectroscopy (EIS) in microbial fuel cell studies, Energy Environ. Sci. 2 (2009) 215-219, https://doi.org/10.1039/B814914C.

[48] V. Madhavi, P. Jeevan Kumar, P. Kondaiah, O.M. Hussain, S. Uthanna, Effect of molybdenum doping on the electrochromic properties of tungsten oxide thin films by RF magnetron sputtering, Ionics 20 (2014) 1737-1745, https://doi.org/10.1007/s11581-014-1073-8.

[49] I. Andersson, J.J. Hastings, O.W. Howarth, L. Pettersson, Aqueous molybdotungstates, J. Chem. Soc. Dalton Trans. (1994) 1061-1066, https://doi.org/10.1039/DT9940001061.

[50] A. Katrib, V. Logie, N. Saurel, P. Wehrer, L. Hilaire, G. Maire, Surface electronic structure and isomerization reactions of alkanes on some transition metal oxides, Surf. Sci. 377 (1997) 754-758, https://doi.org/S0039-6028(96)01488-4.

[51] L. Huang, L. Gan, N. Wang, X. Quan, B.E. Logan, G. Chen, Mineralization of pentachlorophenol with enhanced degradation and power generation from air

cathode microbial fuel cells, Biotechnol. Bioeng. 109 (2012) 2211-2221, https://doi.org/10.1002/bit.24489.
[52] L. Cao, W. Sun, Y. Zhang, S. Feng, J. Dong, Y. Zhang, B.E. Rittmann, Competition for electrons between reductive dechlorination and denitrification, Front. Environ. Sci. Eng. 11 (2017) 14, https://doi.org/10.1007/s11783-017-0959-x.
[53] F. Jiang, Y. Zhang, N. Sun, Z. Liu, Effect of direct current density on microstructure of tungsten coating electroplated from Na_2WO_4-WO_3-$NaPO_3$ system, Appl. Surface Sci. 317 (2014) 867-874, https://doi.org/10.1016/j.apsusc.2014.09.031.
[54] W. Li, H. Yu, Z. He, Towards sustainable wastewater treatment by using microbial fuel cell-centered technologies, Energy Environ. Sci. 7 (2014) 911-924, https://doi.org/10.1039/C3EE43106A.
[55] D. Jafarifar, M.R. Daryanavard, S. Sheibani, Ultra fast microwave-assisted leaching for recovery of platinum from spent catalyst, Hydrometallurgy 78 (2005) 166-171, https://doi.org/10.1016/j.hydromet.2005.02.006.
[56] H.L. Le, J. Jeong, J.C. Lee, B.D. Pandey, J.M. Yoo, T.H. Huyunh, Hydrometallurgical process for copper recovery from waste printed circuit boards (PCBs), Miner. Process. Extr. Metall. Rev. 32 (2011) 90-104, https://doi.org/10.1080/08827508.2010.530720.

Table 1 Separator factors in the 1# and the 2# units under various operational conditions

Fig. 1 Effect of various W concentrations on rates of (A) W and (B) Mo deposition, (D) current, and (E) cathode potential in the stacked BESs. (C) Applied voltage and (F) hydrogen production in the 1# unit of the stacked BESs. (initial Mo(VI) fixed at 1.0 mM, initial pH: 2.0, cathode: SSS in the 1# and CR in the 2# units).

Fig. 2 Effect of various Mo concentrations on rates of (A) W and (B) Mo deposition, (C) current, (D) cathode potential, (E) applied voltage, and (F) hydrogen production in the stacked BESs (initial W(VI) fixed at 1.0 mM, initial pH: 2.0, cathode: SSS in the 1# and CR in the 2# units).

Fig. 3 XPS analysis for (A, C, E and G) W and (B, D, F and H) Mo elements on the cathodes of (A, B, E and F) the 1# and (C, D, G and H) the 2# units at W/Mo molar ratios of (A, B, C and D) 1 : 0.01 or (E, F, G and H) 0.01 : 1 (initial pH: 2.0, cathode: SSS in the 1# and CR in the 2# units).

Fig. 4 EIS analysis at W/Mo molar ratios of (A) 1 : 1, 0.1 : 1, 0.05 : 1 and 0.01 : 1, and (B) 1: 0.01, 1 : 0.05, 1 : 0.1 and 1 : 1 as well as (C) single W or Mo (initial pH: 2.0, cathode: SSS in the 1# and CR in the 2# units).

Fig. 5 Effect of initial pHs on rates of (A) W and (B) Mo deposition, (C) current, (D) cathode potential, (E) applied voltage and (F) hydrogen production in the stacked BESs (W : Mo = 1 : 1; cathode: SSS in the 1# and CR in the 2# units).

Fig. 6 XPS analysis for (A, C, E and G) W and (B, D, F and H) Mo elements on the cathodes of (A, B, C and D) the 1# and (E, F, G and H) the 2# units at an initial pH of (A, B, E and F) 1.5 or (C, D, G and H) 4.0 (W : Mo = 1 : 1, cathode: SSS in the 1# and CR in the 2# units).

Fig. 7 Effect of cathode material on rates of (A) W and (B) Mo deposition, (C) current, (D) cathode potential and (E) applied voltage in the stacked BESs. (F) Rate of hydrogen production in the 1# unit of the stacked BESs (W : Mo = 1 : 1; initial pH: 2.0).

Fig. 8 Rates of (A) W and (B) Mo deposition, (C) current, (D) cathode potential, (E) applied voltage and (F) hydrogen production as a function of equal W/Mo molar ratio (CR in the 1# unit and SSS in the 2 units, initial pH: 2.0).

*Novelty Statement (maximum limit:100 words)

Statement of novelty

W/Mo molar ratio (in the range 0.01 mM : 1 mM and vice-versa), initial pH (1.5 to 4.0), and cathode material (stainless steel mesh, carbon rod and titanium sheet) were revealed for the first time to dramatically impact performance of stacked bioelectrochemical systems composed of microbial electrolysis cell (MEC) serially connected with parallel connected microbial fuel cell (MFC). These impacts were ascribed to the changes in circuital current, cathode potential, voltage output from the MFC applied to the MEC, diffusional resistance and cathode overpotential. Complete metal recovery was achieved at equimolar W/Mo ratio of 0.05 mM : 0.05 mM.

→ Concentration of Mo(VI) more influential than W(VI) on system performance;

→ Complete metal recovery was achieved at equimolar W/Mo ratio of 0.05 mM : 0.05 mM;

→ Acidic pH favored the rates of metal deposition and hydrogen production;

→ Stainless steel mesh, carbon rod and titanium sheet cathodes impacted performance.

*Abstract

Abstract: The deposition and separation of W and Mo from aqueous solutions with simultaneous hydrogen production was investigated in stacked bioelectrochemical systems (BESs) composed of microbial electrolysis cell (1#) serially connected with parallel connected microbial fuel cell (2#). The impact of W/Mo molar ratio (in the range 0.01 mM : 1 mM and vice-versa), initial pH (1.5 to 4.0) and cathode material (stainless steel mesh (SSM), carbon rod (CR) and titanium sheet (TS)) on the BES performance was systematically investigated. The concentration of Mo(VI) was more influential than W(VI) in determining the rate of deposition of both metals and the rate of hydrogen production. Complete metal recovery was achieved at equimolar W/Mo ratio of 0.05 mM : 0.05 mM. The rates of metal deposition and hydrogen production increased at acidic pH, with the fastest rates at pH 1.5. The morphology of the metal deposits and the valence of the Mo were correlated with W/Mo ratio and pH. CR cathodes (2#) coupled with SSM cathodes (1#) achieved a significant rate of hydrogen production (0.82 ± 0.04 $m^3/m^3/d$) with W and Mo deposition (0.049 ± 0.003 mmol/L/h and 0.140 ± 0.004 mmol/L/h (1#); 0.025 ± 0.001 mmol/L/h and 0.090 ± 0.006 mmol/L/h (2#)).

Keywords: Bioelectrochemical system; microbial fuel cell; microbial electrolysis cells; W and Mo deposition; hydrogen production

Table 1

Table 1 Separator factors in the 1# and the 2# units under various operational conditions

	W/Mo molar ratio						
	1 : 0.01	1 : 0.05	1 : 0.1	1 : 1	0.1 : 1	0.05 : 1	0.01 : 1
1#	∞	939 ± 20	717 ± 4	7.4 ± 0.1	5.2 ± 0.8	3.8 ± 0.3	---
2#	∞	605 ± 10	200 ± 8	4.9 ± 0.1	3.3 ± 0.2	2.4 ± 0.1	---
	Initial pH						
	1.5	2.0	2.5	3.0	3.5	4.0	
1#	6.7 ± 0.8	7.4 ± 0.1	5.3 ± 0.3	4.2 ± 0.2	3.1 ± 0.2	2.3 ± 0.3	
2#	4.8 ± 0.5	4.9 ± 0.1	4.5 ± 0.3	3.1 ± 0.1	2.9 ± 0.0	2.1 ± 0.0	
	Cathode material						
	CR-CR	CR-SSS	CR-Ti	SSS-SSS			
1#	4.1 ± 0.7	5.2 ± 0.8	5.7 ± 1.1	7.4 ± 0.1			
2#	4.2 ± 0.1	5.0 ± 0.4	4.7 ± 1.0	4.9 ± 0.0			
	W/Mo molar ratio						
	1 : 1	0.1 : 0.1	0.05 : 0.05				
1#	5.2 ± 0.4	5.6 ± 2.3	1.6 ± 0.2				
2#	5.0 ± 0.2	2.2 ± 0.1	3.7 ± 0.1				

Figure 1

Click here to download high resolution image

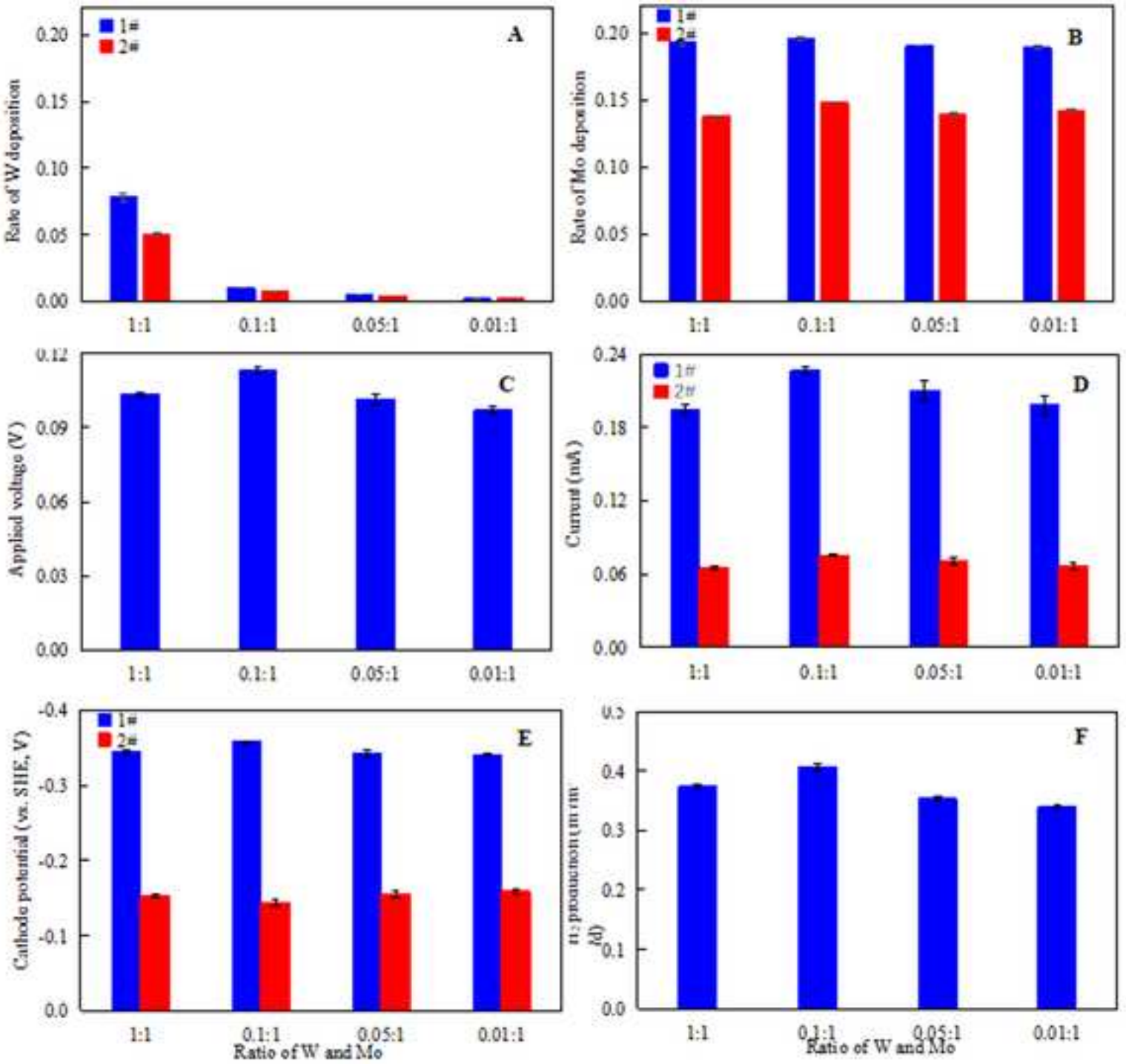

Figure 2

Click here to download high resolution image

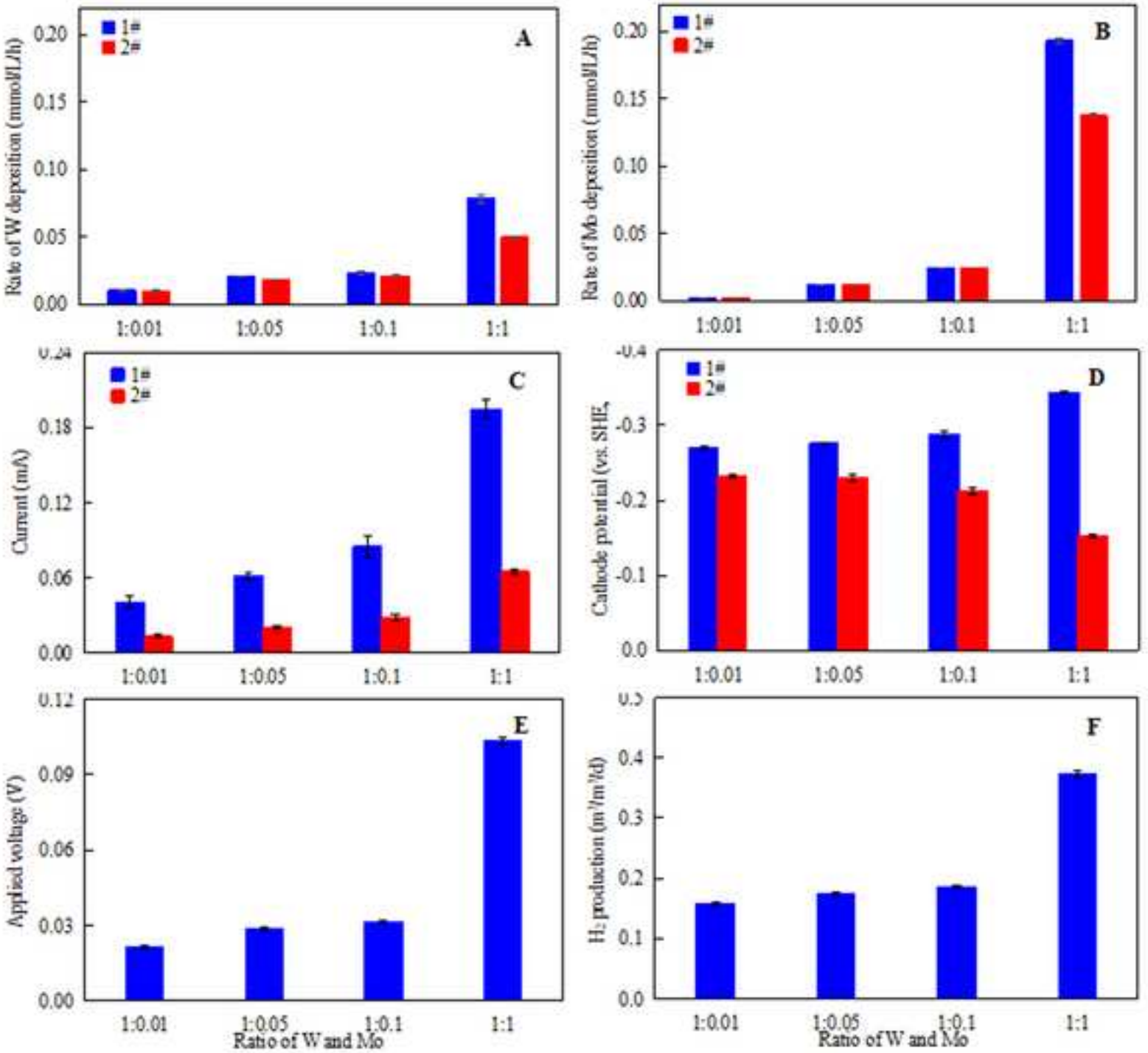

Figure 3

Click here to download high resolution image

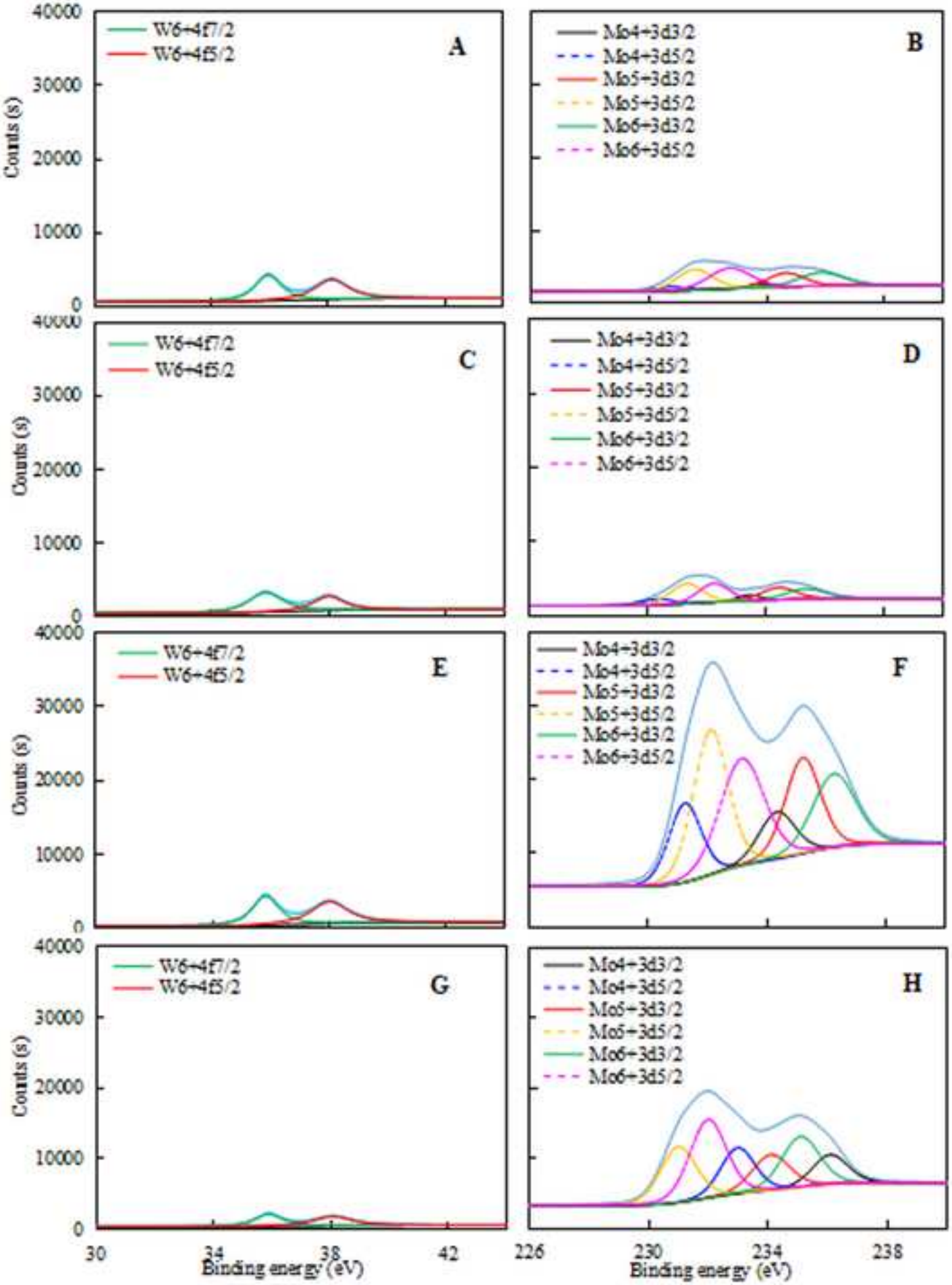

Figure 4

Click here to download high resolution image

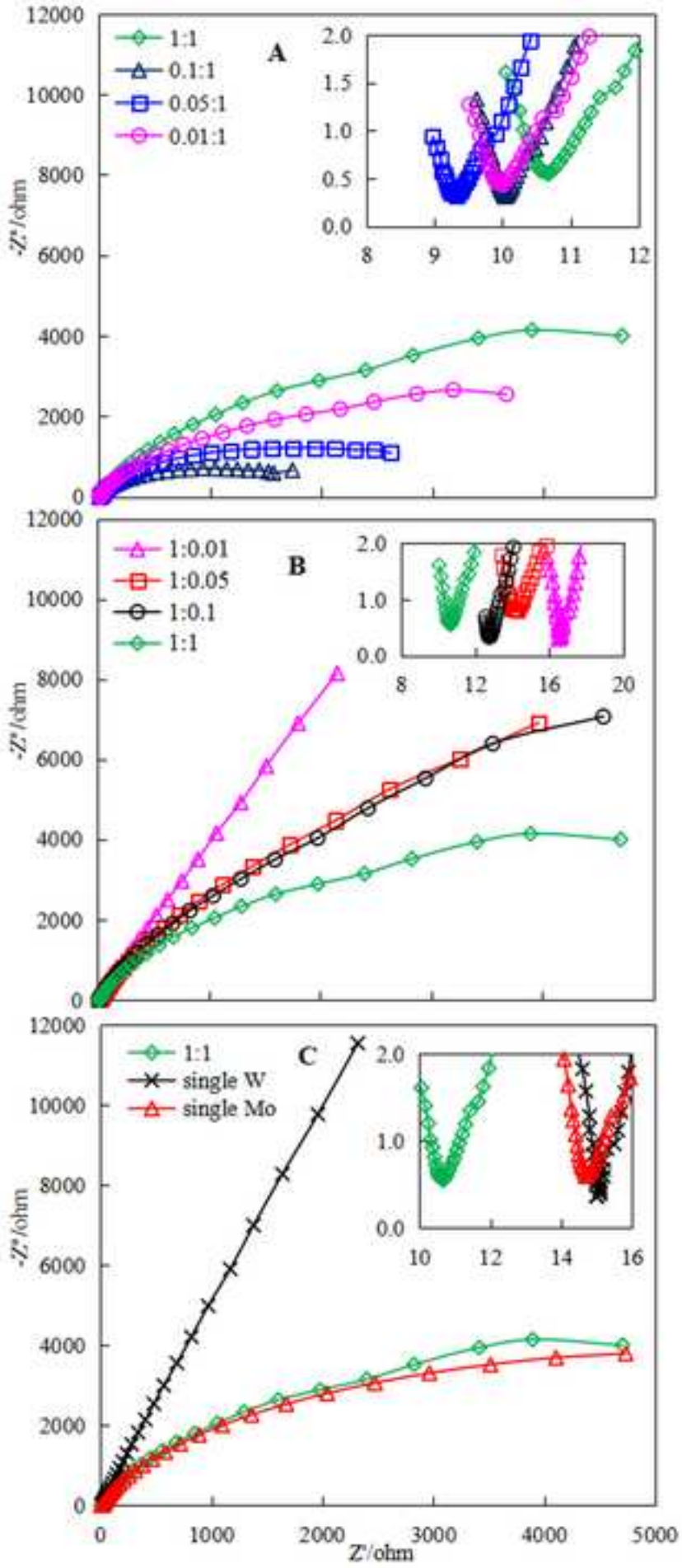

Figure 5

Click here to download high resolution image

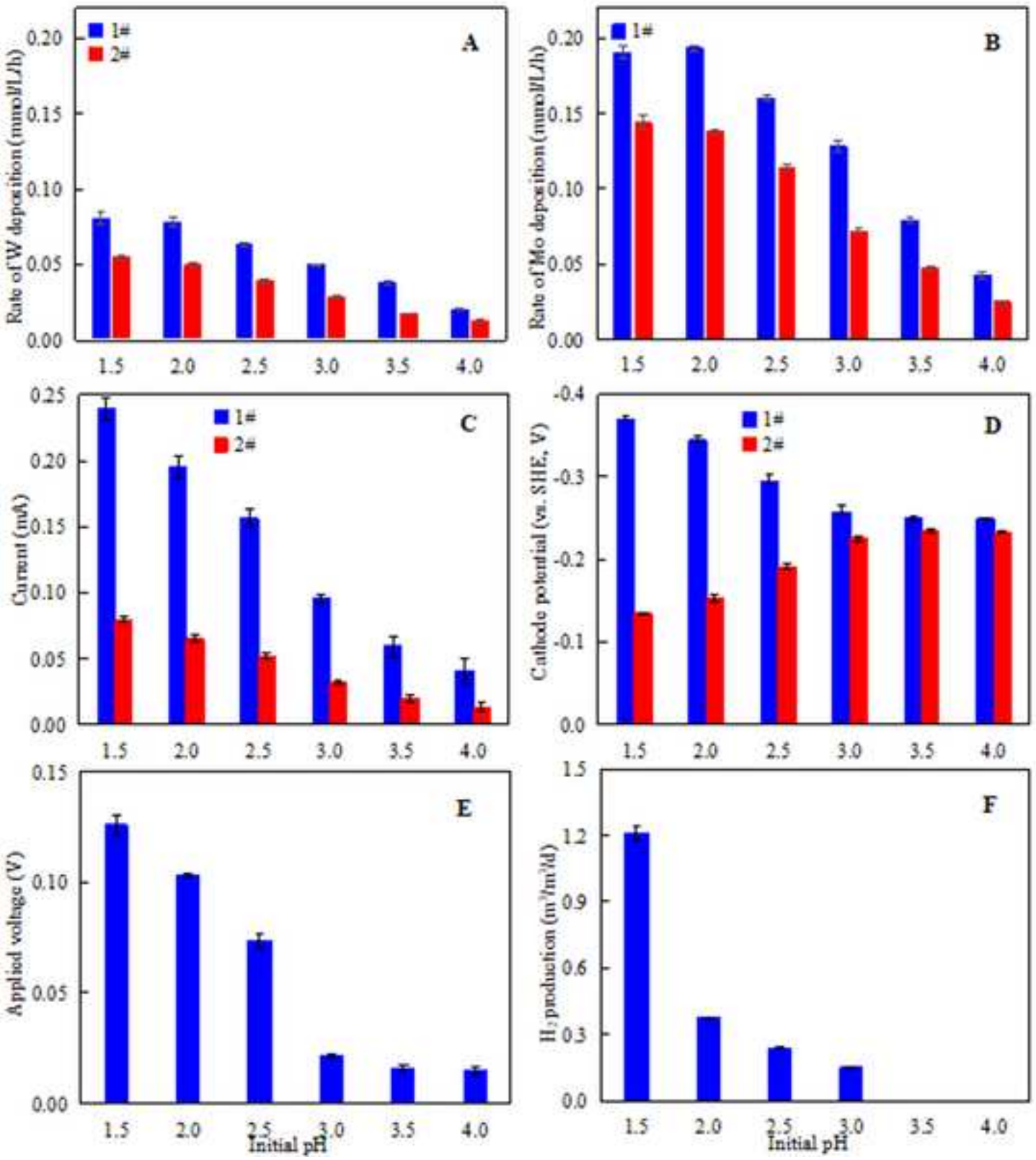

Figure 6

Click here to download high resolution image

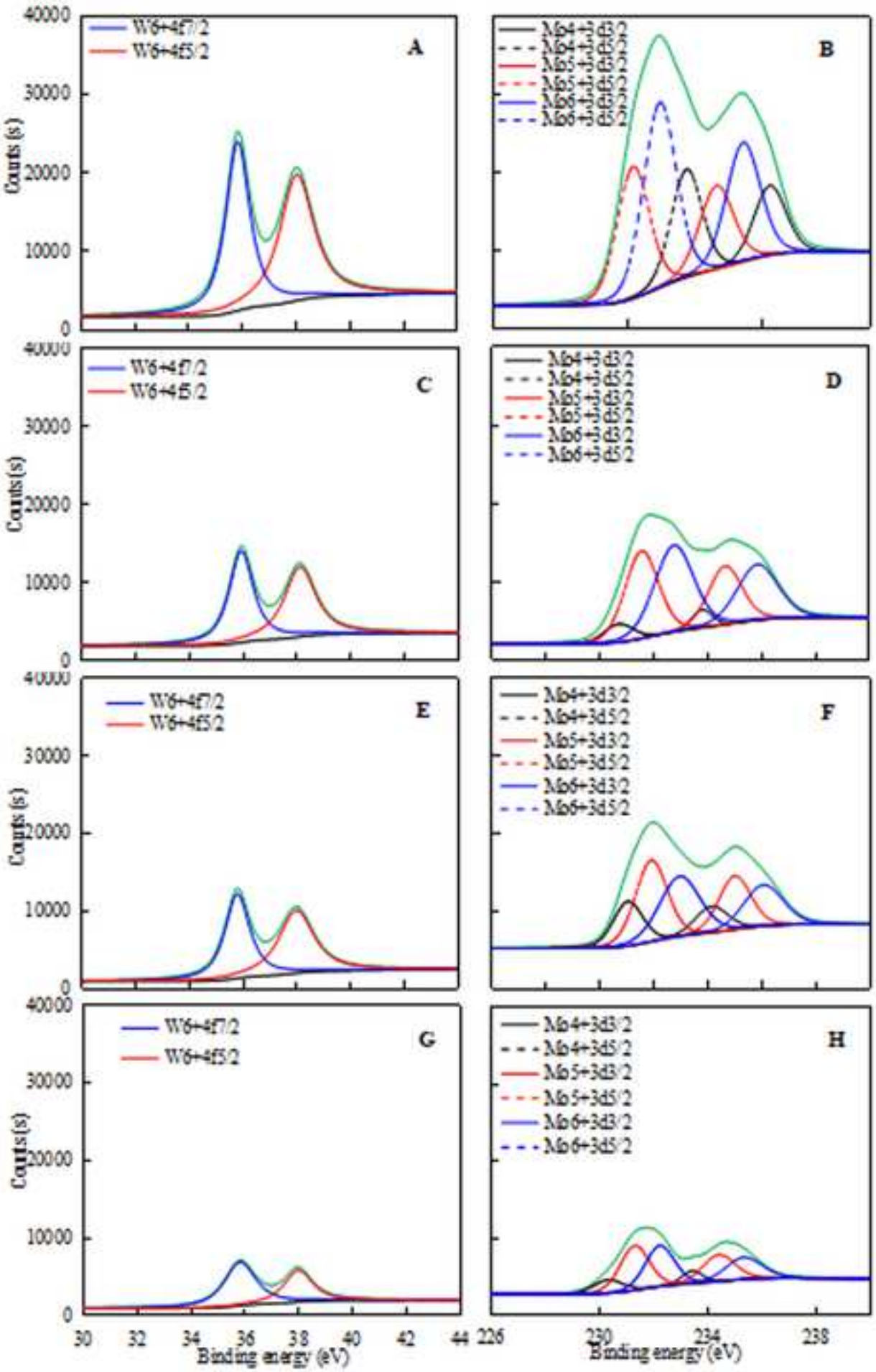

Figure 7

Click here to download high resolution image

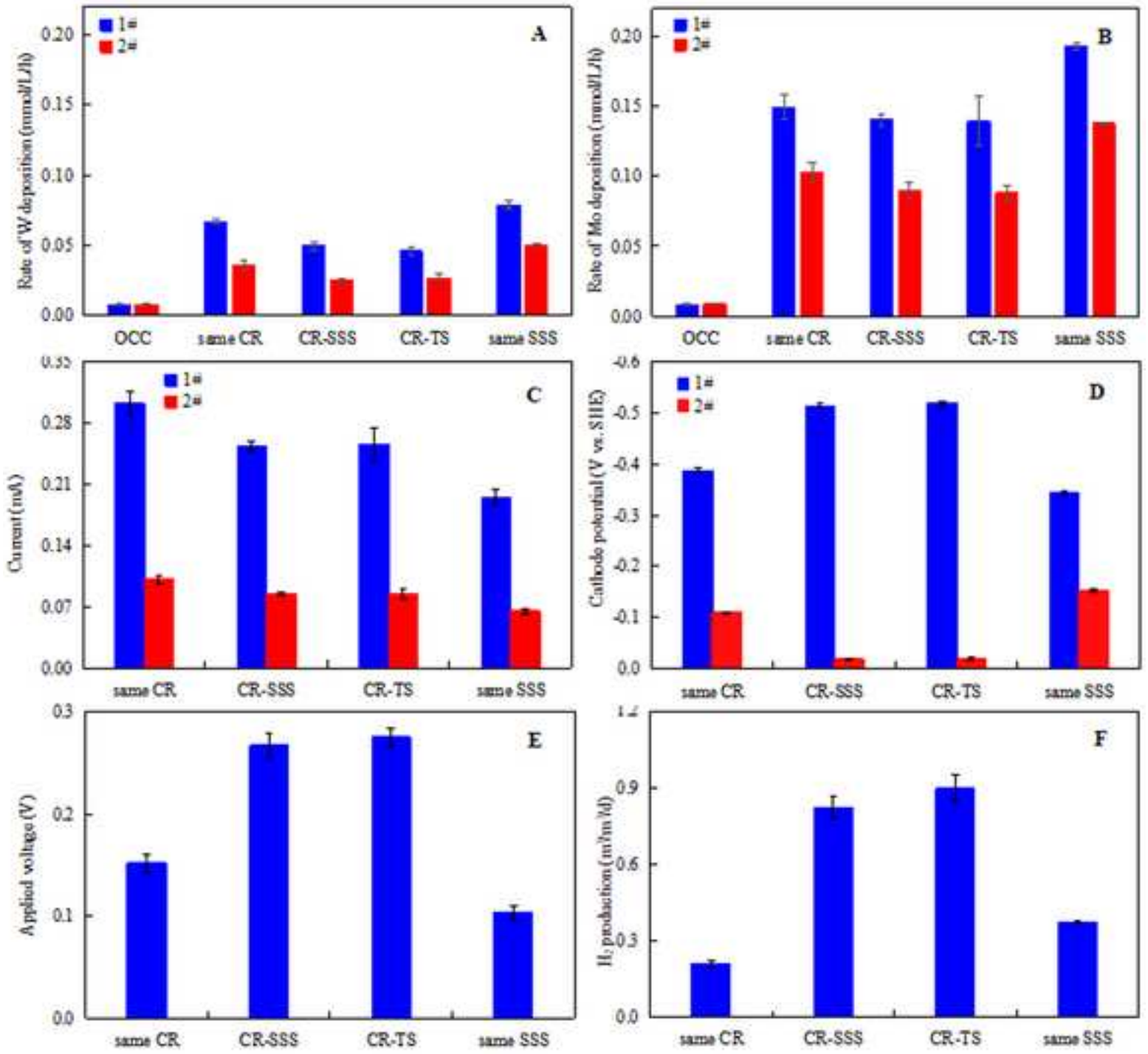

Figure 8

Click here to download high resolution image

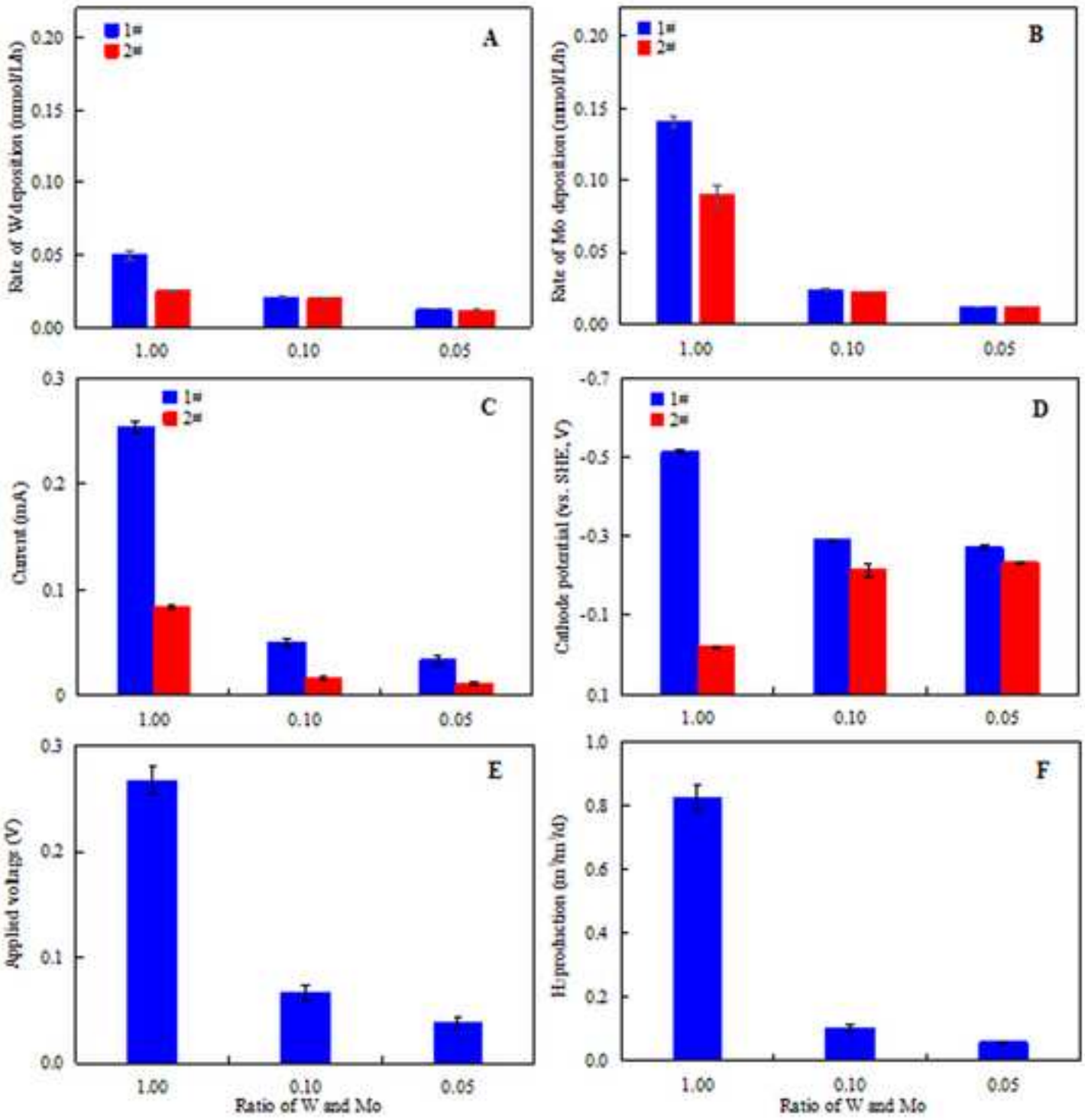

Supplementary Material

Deposition and separation of W and Mo from aqueous solutions with simultaneous hydrogen production in stacked bioelectrochemical systems (BESs): Impact of heavy metals W(VI)/Mo(VI) molar ratio, initial pH and electrode material

Liping Huang[1,*], Ming Li[1], Yuzhen Pan[2], Xie Quan[1], Jinhui Yang[2], Gianluca Li Puma[3,*]

1. Key Laboratory of Industrial Ecology and Environmental Engineering, Ministry of Education (MOE), School of Environmental Science and Technology, Dalian University of Technology, Dalian 116024, China

2. College of Chemistry, Dalian University of Technology, Dalian 116024, China

3. Environmental Nanocatalysis & Photoreaction Engineering, Department of Chemical Engineering, Loughborough University, Loughborough LE11 3TU, United Kingdom

Corresponding authors:

(L. Huang) lipinghuang@dlut.edu.cn

(G. Li Puma) g.lipuma@lboro.ac.uk

The authors declare no competing financial interest.

Pages: 13

Tables: 2

Figures: 9

S2 Materials and Methods

S2.1 Measurements and analyses

$$R_W = \frac{W(VI)_0 - W(VI)_t}{t} \quad \text{(S1)}$$

$$R_{Mo} = \frac{Mo(VI)_0 - Mo(VI)_t}{t} \quad \text{(S2)}$$

$$R_{H_2} = \frac{24 \times \eta_{H_2}}{t} \quad \text{(S3)}$$

$$\varepsilon = \frac{Mo(VI)_0 - Mo(VI)_t}{Mo(VI)_0} \times \frac{W(VI)_t}{W(VI)_0 - W(VI)_t} \quad \text{(S4)}$$

where $W(VI)_0$ and $Mo(VI)_0$ are the initial concentrations (mmol/L) of W(VI) and Mo(VI) in the catholyte of each unit, respectively, and the subscript t refers to the concentration after an operational time of t (h). η_{H2} is the hydrogen concentration (m^3/m^3) at t hours.

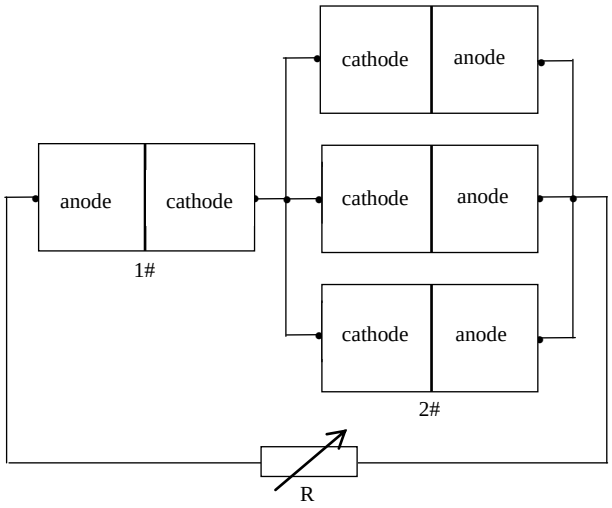

Fig. S1 Schematic diagram of stacked BESs

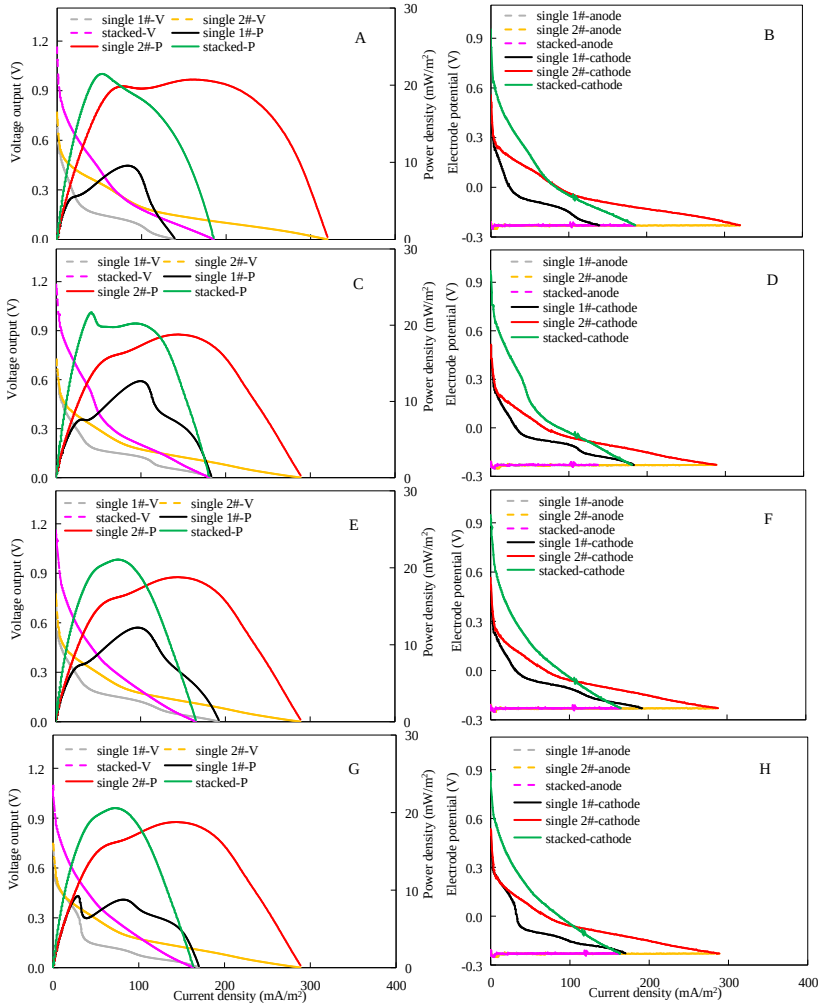

Fig. S2 (A, C, E and G) Polarization curves and (B, D, F and H) electrode potentials of the stacked BESs under various W/Mo molar ratios of (A and B) 1 : 1, (C and D) 0.1 : 1, (E and F) 0.05 : 1, and (G and H) 0.01 : 1.

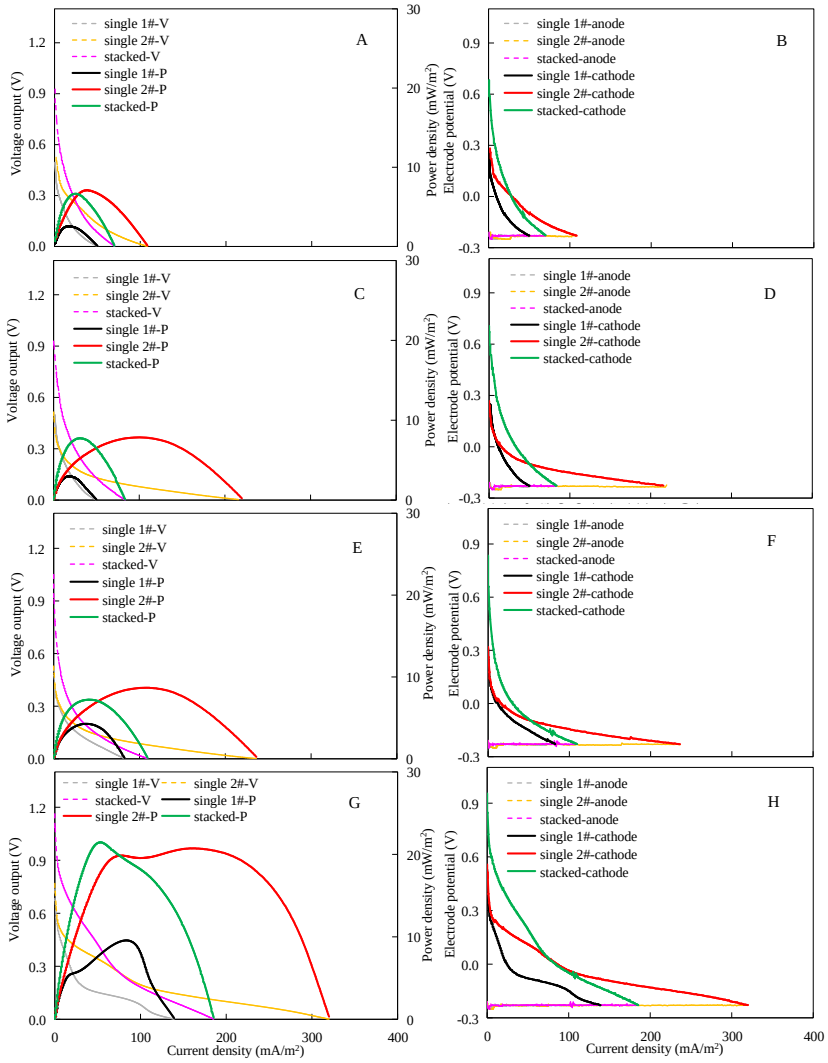

Fig. S3 (A, C, E and G) Polarization curves and (B, D, F and H) electrode potentials of the stacked BESs at various W/Mo molar ratios of (A and B) 1 : 0.01, (C and D) 1 : 0.05, (E and F) 1 : 0.1, and (G and H) 1 : 1.

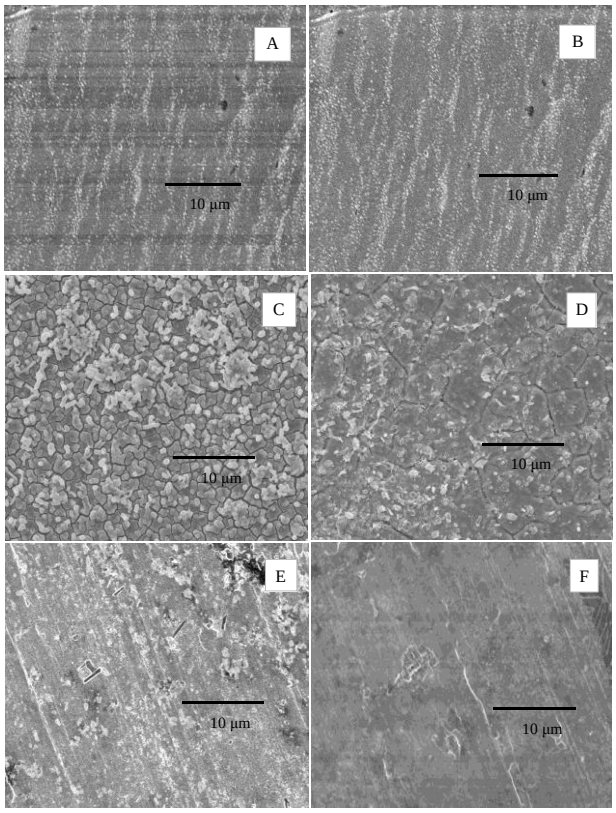

Fig. S4 Morphology of W and Mo deposition on (A, C and E) the 1# unit and (B, D and F) the 2# units of the stacked BESs under W/Mo molar ratios of (A and B) 1 : 0.01, (C and D) 1 : 1, and (E and F) 0.01 : 1.

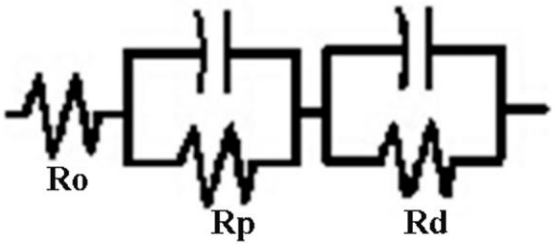

Fig. S5 EIS equivalent circuits.

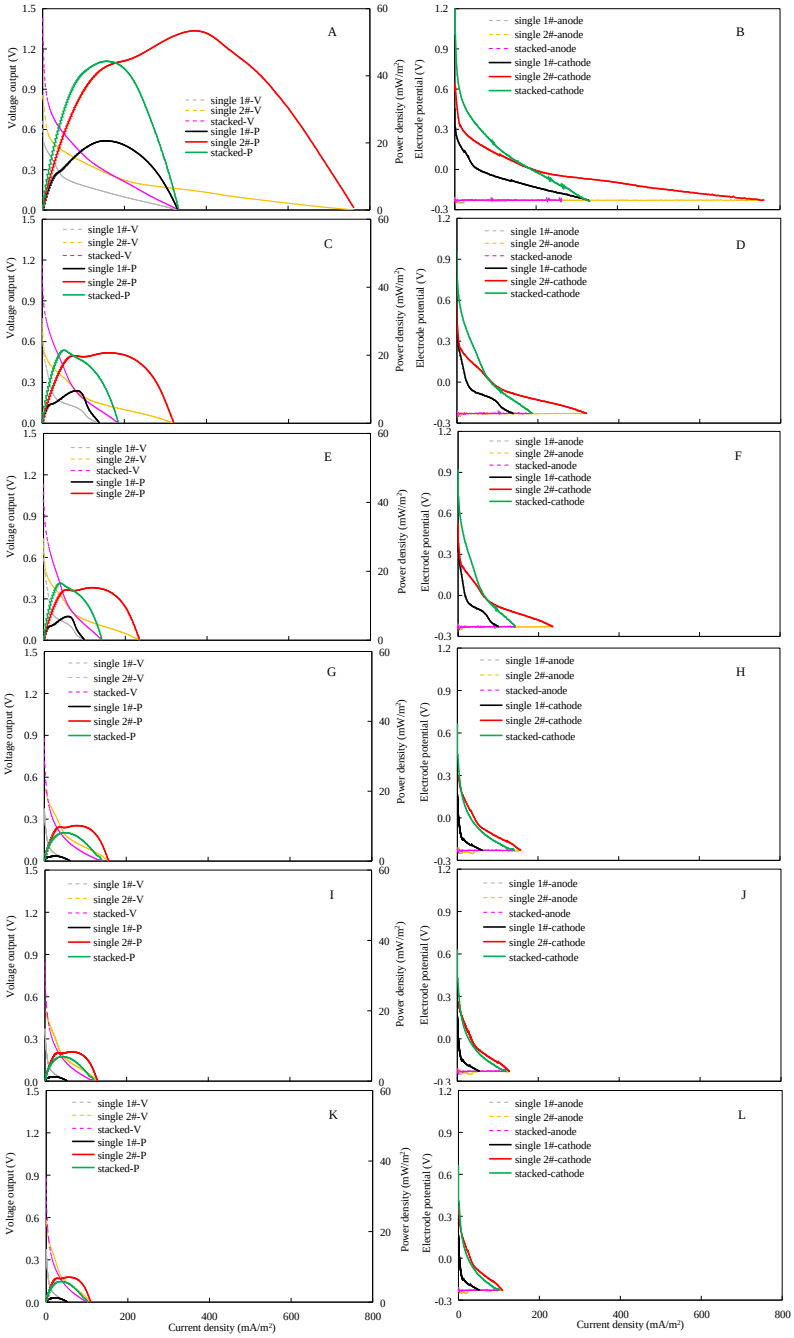

Fig. S6 (A, C, E, G, I and K) Polarization curves and (B, D, F, H, J and L) electrode potentials of the stacked BESs at an initial pH of (A and B) 1.5, (C and D) 2.0, (E and F) 2.5, (G and H) 3.0, (I and J) 3.5, or (K and L) 4.0.

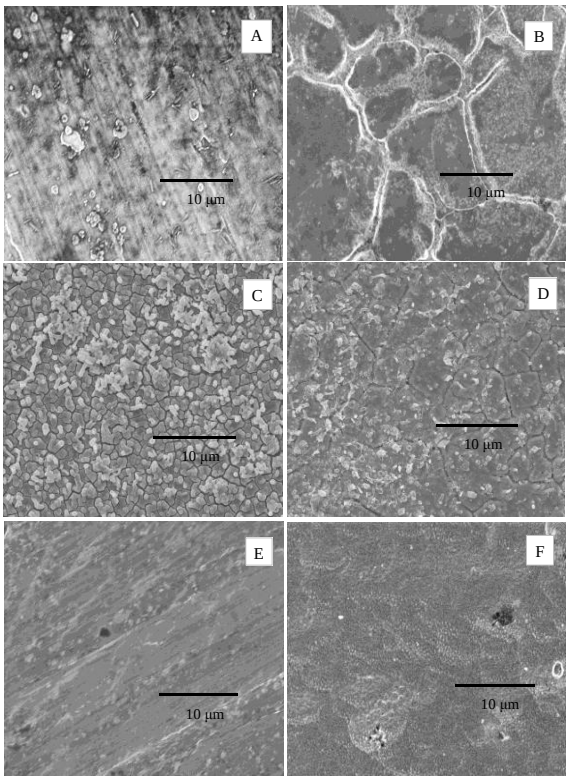

Fig. S7 Morphology of W and Mo deposits on the cathodes of (A, C and E) the 1# and (B, D and F) the 2# units in the stacked BESs at an initial pH of (A and B) 1.5, (C and D) 2.0 or (E and F) 4.0 (W/Mo molar ratio = 1: 1).

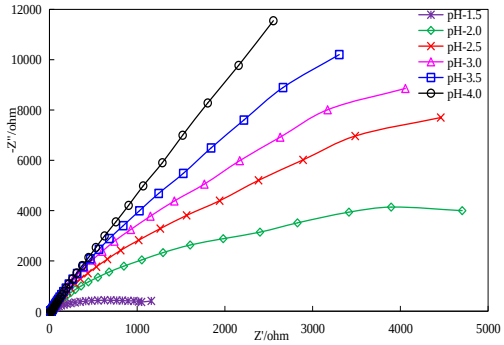

Fig. S8 EIS analysis at various initial pHs (W/Mo molar ratio = 1 : 1, cathode: SSS in the 1# and CR in the 2# units).

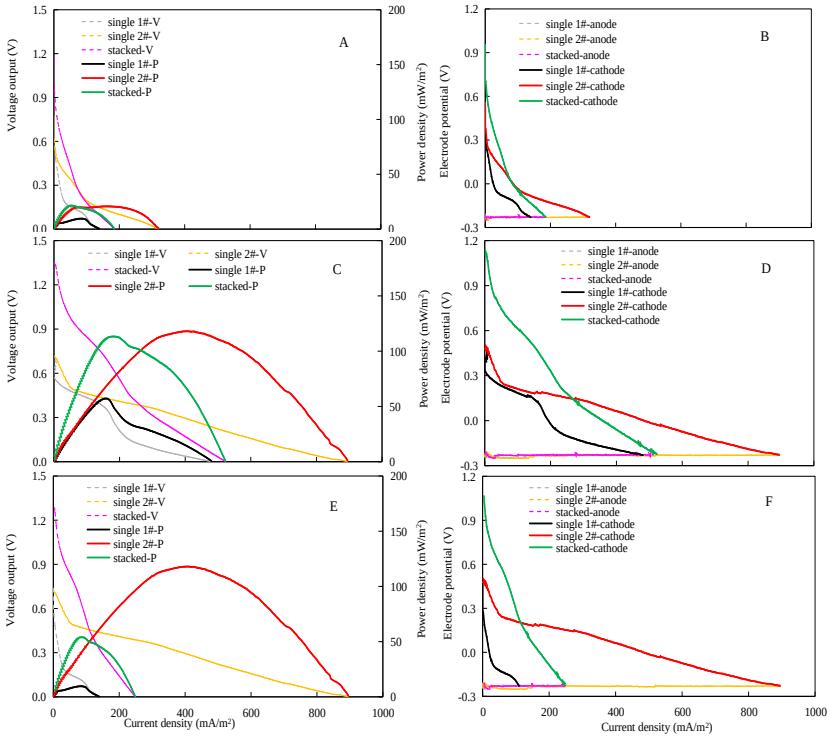

Fig. S9 (A, C and E) Polarization curves and (B, D and F) electrode potentials of the stacked BESs with cathode materials of (A and B) same SSS, (C and D) same CR and (E and F) CR in the 2# unit and SSS in the 1# units (W/Mo molar ratio = 1 : 1; initial pH = 2.0).

Table S1 Molybdenum and tungsten binding energies and corresponding area percent of deposits on cathodes of the 1# and the 2# units in the stacked BESs at various initial pHs or W/Mo molar ratios

Condition		$Mo3d_{3/2}$ (eV)			$Mo3d_{5/2}$ (eV)			$W4f_{5/2}$ (eV)	$W4f_{7/2}$ (eV)	Mo (%)			W (%)
		Mo^{4+}	Mo^{5+}	Mo^{6+}	Mo^{4+}	Mo^{5+}	Mo^{6+}	W^{6+}	W^{6+}	Mo^{4+}	Mo^{5+}	Mo^{6+}	W^{6+}
Initial	1#	233.2	234.5	235.7	230.1	231.4	232.6	37.6	35.4	48	33	19	100
pH 1.5	2#	233.1	234.4	236.0	230.0	231.3	232.9	37.9	35.8	26	41	33	100
Initial	1#	233.1	234.1	235.7	230.0	231.1	232.9	37.9	35.8	13	38	49	100
pH 4.0	2#	233.2	234.5	235.7	230.0	231.0	232.6	37.7	35.6	8	36	56	100
W : Mo =	1#	233.1	234.4	236.0	230.0	231.3	232.9	37.9	35.8	33	45	22	100
0.01 : 1	2#	233.2	234.2	235.7	230.1	230.8	232.2	37.6	35.4	18	38	44	100
W : Mo =	1#	233.1	234.2	236.0	230.0	231.1	232.9	37.7	35.6	12	32	56	100
1 : 0.01	2#	233.2	234.1	235.7	230.1	231.0	232.6	37.6	35.4	4	45	51	100

Table S2 Component analysis of internal resistance of catholyte at various W/Mo molar ratios, and initial pHs.

W : Mo	R_o	R_p	R_d	initial pH	R_o	R_p	R_d
1 : 0.05	16.3	37.7	12810	1.5	6.9	10.1	456
1 : 0.1	14.8	25.7	11500	2.0	11.8	24.9	6744
1 : 1	11.8	24.9	6744	2.5	13.1	30.2	7967
0.1 : 1	10.7	16.6	1548	3.0	13.6	34.9	8976
0.05 : 1	10.1	28.6	2552	3.5	14.9	98.8	10987
0.01 : 1	10.4	37.3	4702	4.0	17.8	121.1	11987
Single W	17.4	134.5	14320				
Single Mo	16.5	64.4	6385				

March 21, 2018

Submitted to J Hazard Mater

Deposition and separation of W and Mo from aqueous solutions with simultaneous hydrogen production in stacked bioelectrochemical systems (BESs): Impact of heavy metals W(VI)/Mo(VI) molar ratio, initial pH and electrode material

Liping Huang[1,*], Ming Li[1], Yuzhen Pan[2], Xie Quan[1], Jinhui Yang[2], Gianluca Li Puma[3,*]

1. Key Laboratory of Industrial Ecology and Environmental Engineering, Ministry of Education (MOE), School of Environmental Science and Technology, Dalian University of Technology, Dalian 116024, China

2. College of Chemistry, Dalian University of Technology, Dalian 116024, China

3. Environmental Nanocatalysis & Photoreaction Engineering, Department of Chemical Engineering, Loughborough University, Loughborough LE11 3TU, United Kingdom

Corresponding authors:

(L. Huang) lipinghuang@dlut.edu.cn

(G. Li Puma) g.lipuma@lboro.ac.uk

The authors declare no competing financial interest.

Abstract: The deposition and separation of W and Mo from aqueous solutions with simultaneous hydrogen production was investigated in stacked bioelectrochemical systems (BESs) composed of microbial electrolysis cell (1#) serially connected with parallel connected microbial fuel cell (2#). The impact of W/Mo molar ratio (in the range 0.01 mM : 1 mM and vice-versa), initial pH (1.5 to 4.0) and cathode material (stainless steel mesh (SSM), carbon rod (CR) and titanium sheet (TS)) on the BES performance was systematically investigated. The concentration of Mo(VI) was more influential than W(VI) in determining the rate of deposition of both metals and the rate of hydrogen production. Complete metal recovery was achieved at equimolar W/Mo ratio of 0.05 mM : 0.05 mM. The rates of metal deposition and hydrogen production increased at acidic pH, with the fastest rates at pH 1.5. The morphology of the metal deposits and the valence of the Mo were correlated with W/Mo ratio and pH. CR cathodes (2#) coupled with SSM cathodes (1#) achieved a significant rate of hydrogen production (0.82 ± 0.04 $m^3/m^3/d$) with W and Mo deposition (0.049 ± 0.003 mmol/L/h and 0.140 ± 0.004 mmol/L/h (1#); 0.025 ± 0.001 mmol/L/h and 0.090 ± 0.006 mmol/L/h (2#)).

Keywords: Bioelectrochemical system; microbial fuel cell; microbial electrolysis cells; W and Mo deposition; hydrogen production

1 Introduction

Tungsten (W) and molybdenum (Mo) transition metals are valuable alloying resources used in various products such as electrochromic materials, gas sensors and lithium ion batteries, in addition to be contained in a range of materials such as special steels and catalysts for petrochemical industries [1-2]. The 2011 annual global production of W and Mo has been reported as 73000 t and 264000 t respectively, with over 80% of W and nearly 40% of Mo being produced in China [3-4]. The extraction of W and Mo from natural ores is an energy intensive process, requiring approximately 11600 kWh/ton of products [5]. The ore dressing wastewater produced during the extraction process of the metals contains a large amount of W and Mo ranging from 10 mg/L to 1000 mg/L, in addition to their existence in the leaching liquor of the spent industrial products [3,6]. The environmental and economic sustainability of the mining process, therefore, requires the recovery and separation of W and Mo from the leaching liquor and from industrial wastewater.

Conventional processes that have been proposed for the extraction and recovery of W and Mo from mining ores include solvent extraction, ion exchange, membrane separation, chemical precipitation and electrochemical treatment [3,7-9]. However, significant challenges remain, including the reduction of the energy consumption and the treatment cost, the reduction of the sludge produced during the treatment and the requirement of bringing the concentration levels of W(VI) and Mo(VI) in the wastewater effluents below the required environmental standards.

This study addresses novel bioelectrochemical systems (BESs) which may

provide an alternative and innovative method for the simultaneous recovery and separation of W and Mo from industrial and mining aqueous effluents [10]. BES multifunctional metallurgical processes have been conceived and intensively investigated, in recent years since they provides cost-effective methods for the extraction and separation of metals [11-12]. In BESs organic matter is oxidized in the anodic chamber while dissolved metals may be simultaneously either reduced in the cathodic chamber or oxidized in the anodic chamber, with the potential of producing free energy [11-14]. BESs operate with zero or minimal external energy consumption, generate very little sludge and require minimal reactor maintenance [15-18]. Multiple metals including V(V), Cr(VI), As(III), Tl (I), Cd(II), Mn(II), Co(II), Ni(II) and Cu(II) [11-12,16,19-27] have been recovered in single units of either microbial fuel cell (MFC) or microbial electrolysis cell (MEC). Differently, stacked metallurgical BESs, configured with MFC units providing in-situ the voltage output to drive the operation of electrically connected MECs, exhibited more merits than single MFC or MEC units. Stacked metallurgical BESs have been conceptually explored for the recovering and separation of multiple metals such as, Cr(VI), Cu(II) and Cd(II), Cu(II) and Co(II), and Cu(II), Co(II) and Li(I) [28-32]. The concept of using optimized MFC and MEC stacked BESs for the efficient deposition and separation of W(VI) and Mo(VI) from mixed aqueous solutions with simultaneous hydrogen production has been demonstrated in our recent study [10] using an initial pH of 2.0, a W(VI)/Mo(VI) molar ratio of 1 : 1 and a stainless steel sheet cathode electrode. However, the impact of the operating parameters require further investigation, in order to optimize the

deposition, separation and recovery of W and Mo metals from practical wastes and wastewaters, with simultaneous hydrogen production.

The concentrations of W(VI) and Mo(VI) in the ores and leaching liquor of spent catalysts are dependent on the characteristics of the mining site or industrial process, with some cases presenting an excess of Mo(VI) and lower amount of W(VI) or vice-versa [4-6,9]. The concentrations of W(VI) and Mo(VI) in the ore dressing wastewater produced during the extraction process, are also closely correlated with the extraction process used. Thus, significant fluctuations in the concentrations of W(VI) and Mo(VI) in the wastewater generally occurs [3,5-6], which translates in variable rates of W and Mo deposition, and thus variable rates of hydrogen production in the MEC units of the stacked BESs. Similarly, pH plays a significant role on the nature of the W and Mo ionic forms present in aqueous solution, on the degree of polymerization of W in electrochemical processes [33], and on the rate of hydrogen evolution in MECs [34-35]. Furthermore, the cathode material also plays an important role. A range of cathodes materials including carbon rod, carbon plate, stainless steel mesh and titanium sheet have been proposed for the recovery of Co(II), Cu(II) and/or Cd(II) in single MFC or MEC units and even stacked BESs [29-31,36-39]. However, the performance of only a few of them has been compared under the same operational conditions [30]. The materials used to recover W and Mo in conventional electrochemical processes operated under galvanic mode include titanium, platinum, nickel, copper and gold [2,40-41]. In particular, W and Mo deposits on these materials also may act as catalysts for the evolution of hydrogen [40-42]. Therefore, the

reduction of heavy metals and the reduction of protons to hydrogen may be competing processes for the cathodic electrons, particularly at low metal concentrations [37-38,43]. Such occurrence may call for the use of different cathodic material and/or experimental conditions depending on the desired treatment objectives.

In this study, stacked BESs were constructed to investigate the impact of the W(VI)/Mo(VI) molar ratio (herein reported as W/Mo for brevity), the initial pH and the cathode electrode material on the rates of W and Mo deposition from aqueous solutions, and on the simultaneous rates of hydrogen production. The W and Mo molar ratio was varied in the range of 0.01 : 1 and vice-versa. The initial pH in the cathodic chamber containing the mixed metals ranged from 1.5 to 4.0, and stainless steel mesh (SSM), carbon rod (CR) and titanium sheet (TS) were systematically explored as cathode materials. The BESs system performance was elucidated by linear sweep voltammetry (LSV), scanning electronic microscopy (SEM), X-ray photoelectron spectroscopy (XPS) and electrochemical impedance spectroscopy (EIS). Cathode potential, current and voltage output from the MFC units applied to the MECs (applied voltage) were employed to assess the rate of W and Mo deposition, the metals separation factor and the rate of hydrogen production. The concept of complete metal recovery was also investigated.

2 Materials and Methods

2.1 BESs assembly

Stacked BESs were designed with one MFC (1#) serially connected with three parallel MFCs (2#) (Fig. S1) as a result of previous optimization of the modules with

multiple units [10]. Each reactor unit was made of two-chambers (14 ml operating volume) separated by a cation exchange membrane (CMI-7000 Membranes International, Glen Rock, NJ). Porous graphite felts (1.0 × 1.0 × 1.0 cm, San Ye Co., Beijing, China) were used as anodes [44], whereas SSS (2.0 × 2.0 cm, Qing Yuan Co., China) were used as the cathodes of both the 1# and the 2# units. A glass tube with an inner diameter of 8 mm was glued to the top of the 1# unit to create a total headspace of 12 mL for hydrogen collection [10,44]. A reference electrode (Ag/AgCl, 195 mV vs. SHE) was installed in the cathodic chamber to measure the electrode potential, with all potentials reported vs. SHE. The reactors were wrapped with aluminum foil to ensure darkness, to avoid the algae growth on the anodes and possible side reactions on the cathodes. The properties of the 2# units have been reported as average values for the sake of clarity, since the differences among the three units connected in parallel were insignificant.

2.2 Inoculation and operation

Anodic inoculation was exactly the same as previously described [28-30]. Mixed W(VI) and Mo(VI) aqueous solutions were prepared using $Na_2WO_4 \cdot 2H_2O$ and $Na_2MoO_4 \cdot 2H_2O$ (Kaida Chemical Co. Ltd., Tianjin, China). The W and Mo molar ratio (mM : mM) in the cathodic chamber was varied as 1 : 1, 0.1 : 1, 0.05 : 1, 0.01 : 1, 1 : 0.1, 1 : 0.05, and 1 : 0.01, and the initial pH was 1.5, 2.0, 2.5, 3.0, 3.5 and 4.0. Also experiments were conducted at equimolar concentrations of 0.1 : 0.1 and 0.05 : 0.05. Solution conductivity was invariably regulated to the maximal 6.60 mS/cm associated with the most acidic pH of 1.5, to exclude the effect of solution

conductivity on system performance [45]. SSM, CR (Chijiu Duratight Carbon Co., Qingdao, China) or TS (Qingyuan Co., China) cathodes (1#) were coupled with SSM or CR cathodes (2#) with equal geometric areas (2.0 × 2.0 cm). The stacked BESs were operated in fed-batch mode at room temperature (25 ± 3 ºC). Three duplicate BESs were used in all experiments.

Control experiments with single W(VI) or Mo(VI) metal in solution were performed to reflect the impact of the binary-component on the system performance. Control experiments under open circuit conditions (OCCs) reflected the effect of current on W and Mo deposition. Other control experiments using the 1# or the 2# units only were performed to illustrate the roles played by each unit on system performance.

2.3 Measurements and analyses

The W(VI) and Mo(VI) concentrations in the catholyte were measured using standard methods [46]. The electrical data were monitored with an automatic data acquisition system (PISO-813, Hongge Co.,Taiwan). The electrical current was calculated from the voltage read across a small external resistance (10 Ω). The hydrogen in the headspace of the cathodic chambers was sampled and analyzed as previously described [10,37-38,44].

The rates of W (R_W, mmol/L/h) and Mo (R_{Mo}, mmol/L/h) deposition on the cathodes was calculated from Eqs. S1 – 2, whereas the power density was normalized to the projected surface area of the separator [10]. The rate of hydrogen production and the separation factor ε were calculated from Eqs. S3 and S4, respectively [10,36].

LSVs were conducted using a potentiostat (CHI 770c, Chenhua, Shanghai) at a scan rate of 1.0 mV/s. The inner resistance of the BES units at different initial pH and W/Mo molar ratios was quantified by EIS (Bio-Logic VMP3) as previously described [10,39,43,47]. The morphologies and valences of the products on the cathode were observed by SEM (Hitachi S-4800) and determined by XPS (Kratos AXIS Ultra DLD). One-way ANOVA in SPSS 19.0 was used to analyze the differences among the data, and all of the data indicated significance levels of $p < 0.05$.

3 Results and discussion

3.1 The impact of W/ Mo molar ratio

At a fixed Mo concentration of 1.0 mM, higher W concentrations favored the deposition of W (Fig. 1A) and negligibly affected the deposition of Mo (Fig. 1B) in both the 1# and the 2# units. The rate of deposition of W was 0.079 ± 0.003 mmol/L/h (1#) and 0.050 ± 0.001 mmol/L/h (2#) (Fig. 1A), while for Mo it was 0.193 ± 0.002 mmol/L/h (1#) and 0.138 ± 0.001 mmol/L/h (2#) (Fig. 1B), at the higher concentration of W investigated (1.0 mM). Greater amounts of W and Mo were invariably deposited in the 1# unit, rather than in the 2# units (Fig. 1A and B), which was ascribed to the voltage output from the 2# units and applied to the 1# unit (Fig. 1C) for the consequent higher currents (Fig. 1D) and more negative cathode potentials (Fig. 1E) in the 1# unit. Higher current and more negative potentials favor the rate of deposition of oxidative metals on the cathodes of BESs [11-12]. The observed polarization curves and electrode potentials as a function of the current (Fig. S2) further demonstrated the significance and impact of the W concentration on the BESs

performance. The similar values of applied voltages, in the range 0.10 – 0.11 V (Fig. 1C), led to the simultaneous evolution of hydrogen at variable rates (0.34 – 0.41 m^3/m^3 d) in the 1# unit, during the deposition of the metals (Fig. 1F). This result also reflected an insignificant effect of W concentrations on the rate of hydrogen production in the 1# unit.

Here Fig. 1

At a fixed W concentration of 1.0 mM, a decrease in Mo concentration decreased the rate of deposition of W (Fig. 2A) and Mo (Fig. 2B) in both the 1# and the 2# units with varying degrees. This resulted in high values of the separation factors equal to 717 ± 4 (1#) and 200 ± 8 (2#), at a W/Mo molar ratio of 1 : 0.1 (Table 1), which were significantly higher than the values (80 to 105) reported in conventional solvent extraction processes [8]. Lower Mo concentrations led to decreased currents (Fig. 2C) and less negative cathode potentials (Fig. 2D) in the 1# unit. It also significantly decreased the applied voltages (Fig. 2E), consistent with the polarization curves and the cathodic potentials as a function of current (Fig. S3), all of which explained the decreased rate of hydrogen production observed (Fig. 2F).

Collectively, the results in Fig. 1 and Fig. 2 show that Mo(VI) was more influential than W(VI) in determining an increase in the rate of deposition of both metals and in the rate of hydrogen production. The influential role of Mo(VI) for either W(VI) recovery or as catalysts for hydrogen evolution in conventional chemical/electrochemical processes has been also shown in other studies [2,7-8,41,48]. Binary mixtures of W(VI) and Mo(VI) reportedly forms diverse molybdotungstates

species, which favor the further deposition of W(VI), however, the deposition of W is inhibited in the absence of Mo(VI) in conventional chemical/electrochemical processes [7,49]. Thus, at high W/Mo molar ratios, the rates of deposition of the metals and hydrogen production were diminished in the stacked BESs.

Here Fig. 2

Here Table 1

The W/Mo molar ratio also influenced the morphology of the metals deposited over the stacked BESs cathodes. Smaller and more homogeneous particles were observed on the cathodes of both the 1# (Fig. S4A) and the 2# (Fig. S4B) units at a W/Mo molar ratio of 1 : 0.01, in comparison to those at a W/Mo ratio of 1 : 1 (Fig. S4C and D). Conversely, a W/Mo molar ratio of 0.01 : 1 led to the presence of irregular deposits in the 1# unit (Fig. S4E) complemented by dense layer deposits in the 2# units (Fig. S4F).

The XPS spectra for the W4f or Mo3d core electronic transitions exhibited the characteristic $4f_{7/2}$ and $4f_{5/2}$ or $3d_{5/2}$ and $3d_{3/2}$ doublet of peaks at 35.8 and 37.9 eV assigned to W(VI) in WO_3 [50], whereas the peaks at 232.9 and 236.0, 231.4 and 234.5, and 230.0 and 233.1 eV corresponded to $Mo3d_{5/2}$ and $Mo3d_{3/2}$ in MoO_3, Mo_2O_5 and MoO_2, respectively (Table S1) [42]. Similar peaks at 35.9 and 38.1 eV were observed in both the 1# (Fig. 3A and E) and the 2# (Fig. 3C and G) units regardless of the W/Mo molar ratio (i.e., high (1 : 0.01) (Fig. 3A and C) or low (0.01 : 1) (Fig. 3E and G)). The catholyte at the end of each fed-batch cycle operation instantly changed in color in the absence of N_2 protection, consistent with the report

that W(V) as a reduced product is highly unstable and easily oxidized to W(VI) due to the sampling procedures [2]. Thus, these similar peaks (Fig. 3A, 3C, 3E and 3G) could presumably be the result from the re-oxidation of the W reduced products. In contrast, the valence of the Mo deposits was strongly correlated with the W/Mo molar ratio and varied among the different units (Fig. 3B, D, F and H). Stronger Mo(V) and Mo(IV) signals were observed at a low W/Mo molar ratio of 0.01 : 1 in the 1# unit (Fig. 3F) rather than in the 2# units (Fig. 3H and Table S1), while much weaker signals were observed at a W/Mo molar ratio of 1 : 0.01 in the 1# unit (Fig. 3B and Table S1). This result demonstrates that Mo(VI) was more easily reduced to Mo(V) rather than Mo(IV).

Here Fig. 3

The variation of the cathode resistances at different W/Mo molar ratios was determined by EIS (Fig. 4) through the fitting of the observed spectra to equivalent electrical circuits (Fig. S5 and Table S2). The ohmic resistance (R_o) at low W/Mo ratios of 0.05 : 1 and 0.01 : 1 was equivalent to that at equimolar W/Mo ratio of 1 : 1, but the polarization resistance (R_p) was higher and the diffusional resistance (R_d) was lower (Fig. 4A and Table S2). Therefore, the deposition of Mo increased the activation loss and decreased the diffusional loss. High W/Mo ratios instead, invariably increased the resistances R_o, R_p and R_d (Fig. 4B and Table S2), consistent with the polarization curves and cathode potentials as a function of current (Fig. S3), implying that the W deposits had a stronger effect than Mo on the resistances. In the control experiments performed with either W(VI) or Mo(VI) in solution, the resistances R_o, R_p and R_d were appreciably higher than those observed with the binary metals (Fig.

4C and Table S2).

Here Fig. 4

3.2 Effect of initial pH

The initial pH of the catholyte was varied in the range from 1.5 to 4.0. At acidic pH of 1.5 and 2.0 the highest rates of W and Mo deposition were observed, equaling 0.0785 ± 0.003 – 0.0808 ± 0.004 mmol/L/h (W) and 0.190 ± 0.004 – 0.193 ± 0.002 mmol/L/h (Mo) in the 1# unit, and 0.0501 ± 0.001 – 0.0548 ± 0.001 mmol/L/h (W) and 0.138 ± 0.001 – 0.144 ± 0.005 mmol/L/h (Mo) in the 2# units (Fig. 5A and B). Higher amounts of metals deposited in the 1# than in the 2# units, were generally accompanied by higher separation factors in the former (Table 1), consistent with the higher currents (Fig. 5C) and the more negative cathode potentials (Fig. 5D) observed in the 1# unit, both of which generally favor the reduction of oxidative substrates [11,51]. A decreasing trend of the rate of metal deposition was observed at an initial pH higher than 2.0.

Smaller polarization loss (Fig. S6), higher applied voltage (Fig. 5E) and an appreciable higher rate of hydrogen production (Fig. 5F) were observed at more acidic initial pH in the 1# unit, consistent with the decrease of the pH in the effluents from 5.93 ± 0.08 at an initial pH of 4.0 to 2.27 ± 0.06 at pH 1.5. Other studies, performed with MECs in the absence of W or/and Mo also reported faster rates of hydrogen production at more acidic pH [34-35]. Considering the similar rates of W and Mo depositions at pH 1.5 and 2.0 (Fig. 5A and B), the significantly higher hydrogen production at pH 1.5 implied that hydrogen evolution outcompeted the

deposition of the metals for the available cathodic electrons, alike the electron competition between reductive dechlorination and denitrification [52].

An experiment with pH controlled at 1.5 during the entire operational period was purposely investigated to determine its effect on the metal deposition. An appreciable higher rate of hydrogen production of 2.14 ± 0.07 $m^3/m^3/d$, and enhanced W and Mo deposition rates (W: 0.0965 ± 0.005 mmol/L/h; Mo: 0.227 ± 0.005 mmol/L/h) in the 1# unit were observed, compared to the results obtained without pH control (1.21 ± 0.03 $m^3/m^3/d$, 0.081 ± 0.004 mmol/L/h (W) and 0.190 ± 0.004 mmol/L/h (Mo)). In concert, the results observed supported a significant dependence of the rate of W and Mo deposition with simultaneous hydrogen production on the pH in the catholyte.

Here Fig. 5

The morphology of the W and Mo deposits was significantly influenced by the initial pH in the catholyte. Wider cracks and larger areas surrounded by the cracks in both the 1# and the 2# units (Fig. S7A and B) were observed at pH 1.5, in comparison to the results at pH 2.0 and 4.0, consistent with the morphology of Mn, Mo and W co-deposits in conventional electrochemical processes [33]. Larger W and Mo grain sizes were consistently observed in the 1# (Fig. S7A, C and E) than in the 2# units (Fig. S7B, D and F), and the grain size was inversely correlated with the increase in the initial pH in the same units. The higher currents observed in the 1# than in the 2# units at the same pH (Fig. 5C) resulted in wider cracks and smaller grains, consistent with the tungsten morphology influenced by current in conventional electrochemical processes [53].

The XPS binding energies (Fig. 6) for Mo and W deposits as well as the corresponding area percent (Table S1) showed that at an initial pH 1.5 appreciable higher Mo(IV) products were achieved in the 1# unit (48%, Fig. 6B and Table S2) than in the 2 units (26%, Fig. 6F and Table S2), both of which were higher than the results at an initial pH of 4.0 (13% in 1#, Fig. 6D and 8% in 2#, Fig. 6H and Table S2). These results clearly demonstrate the dependency of the valences of the Mo deposits on the initial pH. Similarly, the peaks associated with W deposits in the 1# unit at pH 1.5 (Fig. 6A) were apparently higher than either in the 2# units at the same pH (Fig. 6E) or in the same 1# unit but at pH 4.0 (Fig. 6C). The lowest peaks were observed in the 2# units at pH 4.0 (Fig. 6G). Collectively, these results demonstrated a significant dependency of the rate of W and Mo deposition, and even the dependence of the valence of the Mo deposits, on the initial pH of the catholyte, and on the units of the stacked BESs.

Here Fig. 6

EIS spectra were used to identify the components of the internal resistances as a function of the initial pH. R_d, R_p and R_o in concert exhibited increase trends with an increase in the initial pH, from 456 Ω, 10.1 Ω and 6.9 Ω at a pH of 1.5, to 11987 Ω, 121.1 Ω and 17.8 Ω at pH 4.0 (Fig. S8 and Table S2). These results clearly illustrated the favorable effect of acidic pH on decreasing the internal resistances of the stacked BESs, consistent with the results shown in Fig. 5.

3.3 Effect of electrode material

The use of inexpensive SSS cathodes in both the 1# and the 2# units achieved the

highest rate of W (Fig. 7A) and Mo deposition (Fig. 7B) with lower rates of hydrogen production (Fig. 7F) and more polarization loss (Fig. S9A and B), in comparison to the other electrodes combinations tested (Fig. 7A, B and F, Fig. S9). SSS cathodes (1#) coupled with the CR cathodes (2#) exhibited similar more negative cathode potentials and higher currents as the configuration using TS (1# unit) and CR (2#) cathodes (Fig. 7C and D), resulting in higher applied voltages (Fig. 7E) and the subsequent significant rate of hydrogen production of 0.82 ± 0.04 $m^3/m^3/d$ (Fig. 7F) with W and Mo deposition (W: 0.049 ± 0.003 mmol/L/h (1#), 0.025 ± 0.001 mmol/L/h (2#); Mo: 0.140 ± 0.004 mmol/L/h (1#), 0.090 ± 0.006 mmol/L/h (2#)) (Fig. 7A and B). Hydrogen evolution is well known to increase the pH in solution [34], which in consequence penalizes the deposition of W and Mo [10], explaining reduced rates of W and Mo deposition at much more negative cathode potentials and higher currents (Fig. 7A – D). The results collectively show that SSS (1#) and CR (2 #) represent well-matched electrodes for efficient W and Mo deposition in the stacked BESs.

Here Fig. 7

3.4 Complete metal recovery

The results reported have shown that the W(VI)/Mo(VI) molar ratio significantly affected the rate of metals deposition, as well as, the rate of hydrogen production in the stacked BESs. W(VI)/Mo(VI) molar ratios smaller or equal to 1 : 1 favoured the deposition of more W and Mo in the 1# than the 2# units with a negligible effect on the rate of hydrogen production (Fig. 1). In contrast, W(VI)/Mo(VI) molar ratios larger than 1 : 1 resulted in similar rates of deposition of both metals in both the 1#

and the 2# units, and more than halved the rate of hydrogen production (Fig. 2). Further experiments with equimolar W(VI)/Mo(VI) molar ratios and lower initial metals concentrations (1 : 1, 0.1 : 0.1 and 0.05 : 0.05) were performed at an initial pH of 2.0 with cathodes of SSS (1#) and CR (2#) to clarify the role of equimolar heavy metals concentration on system performance. The rates of W (Fig. 8A) and Mo (Fig. 8B) deposition decreased when reducing the concentrations of the metals from 1 : 1 to 0.05 : 0.05. At the lower metals concentrations of 0.05 : 0.05, complete heavy metals deposition was achieved in the 1# unit and almost complete deposition (94.3 ± 2.2% (W) and 98.4 ± 0.8% (Mo)) occurred in the 2# units. Simultaneously, lower separation factors (Table 1), smaller currents (Fig. 8C), more positive cathode potentials (Fig. 8D), lower applied voltages (Fig. 8E) and smaller rates of hydrogen production (Fig. 8F) were observed in comparison to the 1 : 1 case. These results demonstrate the feasibility of these stacked BESs for either complete deposition of W and Mo at this lower equivalent W and Mo concentrations, or higher rates of hydrogen production at higher equivalent W and Mo concentrations.

Here Fig. 8

The deposition of binary mixtures of W(VI) and Mo(VI) in stacked BESs have shown synergistic effects on the recovery of the metals and the simultaneous production of hydrogen [10]. However, the optimization of such BESs required further analysis to account for the impact of fluctuations in the concentration of heavy metals and pH in the wastewater [4-6]. Furthermore, the electrode materials exert a significant impact on the rates of other metals deposition and hydrogen production in

BESs [35,37-37,54]. The elucidation of such effects is required for further optimization of BESs, which could ultimately lead to industrial application.

The present study has illustrated the dependency of rates of W and Mo deposition, as well as, hydrogen production on the W/Mo molar ratio, initial pH and electrode material. Mo(VI) was more influential than W(VI) in determining an increase in the rates of deposition of both metals and hydrogen production. The merit of completely depositing W and Mo at an initial equimolar W/Mo ratio of 0.05 : 0.05 gives an advantage of this technology over conventional methods such as ion exchange, chemical precipitation or adsorption [5,9], particularly with low-strength W and Mo wastewaters from either the mining industry processes or wastewater effluents. Such lower concentrations of metals in high strength wastewater could be achieved with the partial recirculation of the effluent back to the influent [55-56] to dilute the feed stream to the stacked BESs to optimal values, achieving enhanced metal deposition and even complete separation of W and Mo (Fig. 1,2 and 8, and Table 1). Practical implementation will also depend on the long-term operation of this system, as well as, the process economics of BESs relative to conventional treatment processes [54]. Although the present economic values of W and Mo deposits are relatively low, the added complexity in the stacked BESs will be paid off with increasing the demand on sustainability and elevated product values due to the depletion of W and Mo resources. The simultaneous production of hydrogen by-product in the MEC units of the stacked BESs further offsets the cost of this technology, although further pilot and full-scale investigations are necessary to

evaluate the long-term operation and stability of the system over feeds with fluctuating physico/chemical properties.

4 Conclusions

Stacked BESs composed of MEC (1#) serially connected with parallel connected MFC (2#) have been shown to be effective in W and Mo deposition and separation with simultaneous hydrogen production. It revealed a dramatic effect of the W/Mo molar ratio, initial pH, and cathode material on the rates observed. The concentration of Mo(VI) was more influential than W(VI) in determining the rate of deposition of both metals and the rate of hydrogen production. Complete metal recovery was achieved at equimolar W/Mo ratio of 0.05 mM : 0.05 mM. Acidic pH favored both the deposition of the metals and the rate of hydrogen production. The BESs comprising CR cathodes (2#) coupled with SSS cathodes (1#) achieved optimal performance. The BESs studied here may provide an alternative and innovative method for the recovery and separation of W and Mo from industrial and mining aqueous effluents with simultaneous hydrogen production.

Acknowledgments

The authors are gratefully acknowledge financial support from the National Natural Science Foundation of China (Nos. 51578104 and 21777017), and the Programme of Introducing Talents of Discipline to Universities (B13012).

References

[1] D. Merki, X. Hu, Recent developments of molybdenum and tungsten sulfides as hydrogen evolution catalysts, Energy Environ. Sci. 4 (2011) 3878-3888, http://dx.doi.org/10.1039/C1EE01970H.

[2] S. Sun, T. Bairachna, E.J. Podlaha, Induced codeposition behavior of electrodeposited NiMoW alloys, J. Electrochem. Soc. 160 (2013) D434-D440, http://dx.doi.org/10.1149/2.014310jes.

[3] T.A. Lasheen, M.E. El-Ahmady, H.B. Hassib, A.S. Helal, Molybdenum metallurgy review: Hydrometallurgical routes to recovery of molybdenum from ores and mineral raw materials, Miner. Process. Extr. Metall. Rev. 36 (2015)145-173, http://dx.doi.org/10.1080/08827508.2013.868347.

[4] T. Ogi, T. Makino, K. Okuyama, W.J. Stark, F. Iskandar, Selective biosorption and recovery of tungsten from an urban mine and feasibility evaluation, Ind. Eng. Chem. Res. 55 (2016) 2903-2910, http://dx.doi.org/10.1021/acs.iecr.5b04843.

[5] Z. Zhao, C. Cao, X. Chen, G. Huo, Separation of macro amounts of tungsten and molybdenum by selective precipitation, Hydrometallurgy 108 (2011) 229-232, https://doi.org/10.1016/j.hydromet.2011.04.006.

[6] R.R. Srivastava, N.K. Mittal, B. Padh, B. Ramachandra Reddy, Removal of tungsten and other impurities from spent HDS catalyst leach liquor by an adsorption route, Hydrometallurgy 127-128 (2012) 77-83, https://doi.org/10.1016/j.hydromet.2012.07.004.

[7] L. Kondrachova, P.H. Benjamin, G. Vijayaraghavan, R.D. Williams, K.J. Stevenson, Cathodic electrodeposition of mixed molybdenum tungsten oxides from peroxo-polymolybdotungstate solutions, Langmuir 22 (2006) 10490-10498, https://doi.org/10.1021/la061299n.

[8] W. Guan, G. Zhang, C. Gao, Solvent extraction separation of molybdenum and tungsten from ammonium solution by H_2O_2-complexation, Hydrometallurgy 127-128 (2012) 84-90, https://doi.org/10.1016/j.hydromet.2012.07.008.

[9] G. Huo, C. Peng, Q. Song, X. Lu, Tungsten removal from molybdate solutions using ion exchange, Hydrometallurgy 147-148 (2014) 217-222, https://doi.org/10.1016/j.hydromet.2014.05.015.

[10] L. Huang, M. Li, Y. Pan, Y. Shi, X. Quan, G. Li Puma, Efficient W and Mo deposition and separation with simultaneous hydrogen production in stacked bioelectrochemical systems, Chem. Eng. J. 327 (2017) 584-596, http://dx.doi.org/10.1016/j.cej.2017.06.149.

[11] H. Wang, Z.J. Ren, Bioelectrochemical metal recovery from wastewater: a review, Water Res. 66 (2014) 219-232, http://dx.doi.org/10.1016/j.waters.2014.08.013.

[12] Y.V. Nancharaiah, S.Venkata Mohan, P.N.L. Lens, Biological and bioelectrochemical recovery of critical and scarce metals, Trends Biotechnol. 34 (2016) 137-155, http://dx.doi.org/10.1016/j.tibtech.2015.11.003.

[13] X. Yong, D. Gu, Y. Wu, Z. Yan, J. Zhou, X. Wu, P. Wei, H. Jia, T. Zheng, Y. Yong, Bio-electron-fenton (BEF) process driven by microbial fuel cells for triphenyltin chloride (TPTC) degradation, J. Hazard. Mater. 324 (2017) 178-183, http://dx.doi.org/10.1016/j.jhazmat.2016.10.047.

[14] Q. Zhao, H. Yu, W. Zhang, F.T. Kabutey, J. Jiang, Y. Zhang, K. Wang, J. Ding, Microbial fuel cell with high content solid wastes as substrates: a review, Front. Environ. Sci. Eng. 11 (2017) 13, http://dx.doi.org/10.1007/s11783-017-0918-6.

[15] O. Modin, X. Wang, X. Wu, S. Rauch, K.K. Fedje,

Bioelectrochemical recovery of Cu, Pb, Cd, and Zn from dilute solutions, J. Hazard. Mater. 235 (2012) 291-297, http://dx.doi.org/10.1016/j.jhazmat.2012.07.058.
[16] M. Peiravi, S.R. Mote, M.K. Mohanty, J. Liu, Bioelectrochemical treatment of acid mine drainage (AMD) from an abandoned coal mine under aerobic condition, J. Hazard. Mater. 333 (2017) 329-338, http://dx.doi.org/10.1016/j.jhazmat.2017.03.045.
[17] O. Modin, F. Aulenta, Three promising applications of microbial electrochemistry for the water sector, Environ. Sci.: Water Res. Technol. 3 (2017) 391-402, http://dx.doi.org/10.1039/C6EW00325G.
[18] M. Wang, Q. Tan, J.F. Chiang, J. Li, Recovery of rare and precious metals from urban mines-A review, Front. Environ. Sci. Eng. 11 (5) (2017) 1, http://dx.doi.org/10.1007/s11783-017-0963-1.
[19] B. Zhang, C. Feng, J. Ni, J. Zhang, W. Huang, Simultaneous reduction of vanadium (V) and chromium (VI) with enhanced energy recovery based on microial fuel cell technology, J. Power Sources 204 (2012) 34-39, http://dx.doi.org/10.1016/j.jpowsour.2012.01.013.
[20] H. Luo, G. Liu, R. Zhang, Y. Bai, S. Fu, Y. Hou, Heavy metal recovery combined with H_2 production from artificial acid mine drainage using the microbial electrolysis cell, J. Hazard. Mater. 270 (2014) 153-159, http://dx.doi.org/10.1016/j.jhazmat.2014.01.050.
[21] N. Colantonio, Y. Kim, Cadmium (II) removal mechanisms in microbial electrolysis cells, J. Hazard. Mater. 311 (2016) 134-141, http://dx.doi.org/10.1016/j.jhazmat.2016.02.062.
[22] Y. Li, B. Zhang, M. Cheng, Y. Li, L. Hao, Spontaneous arsenic (III) oxidation with bioelectricity generation in single-chamber microbial fuel cells, J. Hazard. Mater. 306 (2016) 8-12, http://dx.doi.org/10.1016/j.jhazmat.2015.12.003.
[23] Y. Dong, J.F. Liu, M.R. Sui, Y.P. Qu, J.J. Ambuchi, H.M. Wang, Y.J. Feng, A combined microbial desalination cell and electrodialysis system for copper-containing wastewater treatment and high-salinity-water desalination, J. Hazard. Mater. 321 (2016) 307-315, http://dx.doi.org/10.1016/j.jhazmat.2016.08.034.
[24] D. Wu, L. Huang, X. Quan, G. Li Puma, Electricity generation and bivalent copper reduction as a function of operation time and cathode electrode material in microbial fuel cells, J. Power Sources 307 (2016) 705-714, https://doi.org/10.1016/j.jpowsour.2016.01.022.
[25] R. Qiu, B. Zhang, J. Li, Q. Lv, S. Wang, Q. Gu, Enhanced vanadium (V) reduction and bioelectricity generation in microbial fuel cells with biocathode, J. Power Sources 359 (2017) 379-383, http://dx.doi.org/10.1016/j.jpowsour.2017.05.099.
[26] G. Wang, B. Zhang, S. Li, M. Yang, C. Yin, Simultaneous microbial reduction of vanadium (V) and chromium (VI) by *Shewanella loihica* PV-4, Bioresour. Technol. 227 (2017) 353-358, http://dx.doi.org/10.1016/j.jpowsour.2017.05.099.
[27] Z. Wang, B. Zhang, Y. Jiang, Y. Li, C. He, Spontaneous thallium (I) oxidation with electricity generation in single-chamber microbial fuel cells, Appl. Energy 209

(2018) 33-42, http://dx.doi.org/10.1016/j.apenergy.2017.10.075.
[28] J. Shen, Y. Sun, L. Huang, J. Yang, Microbial electrolysis cells with biocathodes and driven by microbial fuel cells for simultaneous enhanced Co(II) and Cu(II) removal, Front. Environ. Sci. Eng. 9 (2015) 1084-1095, http://dx.doi.org/10.1007/s11783-015-0805-y.
[29] Y. Zhang, L. Yu, D. Wu, L. Huang, P. Zhou, X. Quan, G. Chen, Dependency of simultaneous Cr(VI), Cu(II) and Cd(II) reduction on the cathodes of microbial electrolysis cells self-driven by microbial fuel cells, J. Power Sources 273 (2015) 1103-1113, https://doi.org/10.1016/j.jpowsour.2014.09.126.
[30] D. Wu, Y. Pan, L. Huang, X. Quan, J. Yang, Comparison of Co(II) reduction on three different cathodes of microbial electrolysis cells driven by Cu(II)-reduced microbial fuel cells under various cathode volume conditions, Chem. Eng. J. 266 (2015) 121-132, https://doi.org/10.1016/j.cej.2014.12.078.
[31] D. Wu, Y. Pan, L. Huang, P. Zhou, X. Quan, H. Chen, Complete separation of Cu(II), Co(II) and Li(I) using self-driven MFCs-MECs with stainless steel mesh cathodes under continuous flow conditions, Sep. Purif. Technol. 147 (2015) 114-124, http://dx.doi.org/10.1016/j.seppur.2015.04.016.
[32] M. Li, Y. Pan, L. Huang, Y. Zhang, J. Yang, Continuous flow operation with appropriately adjusting composites in influent for recovery of Cr(VI), Cu(II) and Cd(II) in self-driven MFC-MEC system, Environ. Technol. 38 (2017) 615-628, http://dx.doi.org/10.1080/09593330.2016.1205149.
[33] N.A. Abdel Ghany, S. Meguro, N. Kumagai, K. Asami, K. Hashimoto, Adodically deposited Mn-Mo-Fe oxide anodes for oxygen evolution in hot seawater electrolysis, Mater. Trans. 44 (2003) 2114-2123.
[34] Y. Ruiz, J.A. Baeza, A. Guisasola, Enhanced performance of bioelectrochemical hydrogen production using a pH control strategy, ChemSusChem 8 (2015) 389-397, http://dx.doi.org/10.1002/cssc.201403083.
[35] A. Kadier, M. Sahaid Kalil, P. Abdeshahian, K. Chandrasekhar, A. Mohamed, N. Farhana Azman, W. Logroño, Y. Simayi, A. Abdul Hamid, Recent advances and emerging challenges in microbial electrolysis cells (MECs) for microbial production of hydrogen and value-added chemicals, Renew. Sust. Energ. Rev. 61 (2016) 501-525, https://doi.org/10.1016/j.rser.2016.04.017.
[36] L. Huang, B. Yao, D. Wu, X. Quan, Complete cobalt recovery from lithium cobalt oxide in self-driven microbial fuel cell-microbial electrolysis cell systems, J. Power Sources 259 (2014) 54-64, https://doi.org/10.1016/j.jpowsour.2014.02.061.
[37] Q. Wang, L. Huang, H. Yu, X. Quan, Y. Li, G. Fan, L. Li, Assessment of five different cathode materials for Co(II) reduction with simultaneous hydrogen evolution in microbial electrolysis cells, Inter. J. Hydrogen Energy 40 (2015) 184-196, https://doi.org/10.1016/j.ijhydene.2014.11.014.
[38] Q. Wang, L. Huang, Y. Pan, P. Zhou, X. Quan, B.E. Logan, H. Chen, Cooperative cathode electrode and in situ deposited copper for subsequent enhanced Cd(II) removal and hydrogen evolution in bioelectrochemical systems, Bioresour. Technol. 200 (2016) 565-571, https://doi.org/10.1016/j.biortech.2015.10.084.
[39] Q. Wang, L. Huang, Y. Pan, X. Quan, G. Li Puma, Impact of Fe(III) as an

effective mediator for enhanced Cr(VI) reduction in microbial fuel cells: Reduction of diffusional resistances and cathode overpotentials, J. Hazard. Mater. 321 (2017) 896-906, http://dx.doi.org/10.1016/j.jhazmat.2016.10.011.

[40] N. Tsyntsaru, H. Cesiulis, M. Donten, J. Sort, E. Pellicer, E.J. Podlaha-Murphy, Modern trends in tungsten alloys electrodeposition with iron group metals, Surface Eng. Appl. Electrochem. 48 (2012) 491-520, http://dx.doi.org/10.3103/S1068375512060038.

[41] T.G. Kelly, S.T. Hunt, D.V. Esposito, J.G. Chen, Monolayer palladium supported on molybdenum and tungsten carbide substrates as low-cost hydrogen evolution reaction (HER) electrocatalysts, Inter. J. Hydrogen Energy 38 (2013) 5638-5644, https://doi.org/10.1016/j.ijhydene.2013.02.116.

[42] M. Zhang, D. Lu, G. Yan, J. Wu, J. Yang, Fabrication of Mo+N-codoped TiO_2 nanotube arrays by anodization and sputtering for visible light-induced photoelectrochemical and photocatalytic properties, J. Nanomater. 2013 (2013) 1-9, http://dx.doi.org/10.1155/2013/648346.

[43] Q. Wang, L. Huang, X. Quan, Q. Zhao, Preferable utilization of in-situ produced H_2O_2 rather than externally added for efficient deposition of tungsten and molybdenum in microbial fuel cells, Electrochim. Acta 247C (2017) 880-890, https://doi.org/10.1016/j.electacta.2017.07.079.

[44] Y. Chen, J. Shen, L. Huang, Y. Pan, X. Quan, Enhanced Cd(II) removal with simultaneous hydrogen production in biocathode microbial electrolysis cells in the presence of acetate or $NaHCO_3$, Inter. J. Hydrogen Energy 41 (2016) 13368-13379, https://doi.org/10.1016/j.ijhydene.2016.06.200.

[45] B.E. Logan, Essential data and techniques for conducting microbial fuel cell and other types of bioelectrochemical system experiments, ChemSusChem 5 (2012) 988-994, https://doi.org/10.1002/cssc.201100604.

[46] American Public Health Association, American Water Works Association, Water Pollution Control Federation, Standard methods for the examination of water and wastewater, *20*th edn. American Public Health Association, Washington, 1998.

[47] Z. He, F. Mansfeld, Exploring the use of electrochemical impedance spectroscopy (EIS) in microbial fuel cell studies, Energy Environ. Sci. 2 (2009) 215-219, https://doi.org/10.1039/B814914C.

[48] V. Madhavi, P. Jeevan Kumar, P. Kondaiah, O.M. Hussain, S. Uthanna, Effect of molybdenum doping on the electrochromic properties of tungsten oxide thin films by RF magnetron sputtering, Ionics 20 (2014) 1737-1745, https://doi.org/10.1007/s11581-014-1073-8.

[49] I. Andersson, J.J. Hastings, O.W. Howarth, L. Pettersson, Aqueous molybdotungstates, J. Chem. Soc. Dalton Trans. (1994) 1061-1066, https://doi.org/10.1039/DT9940001061.

[50] A. Katrib, V. Logie, N. Saurel, P. Wehrer, L. Hilaire, G. Maire, Surface electronic structure and isomerization reactions of alkanes on some transition metal oxides, Surf. Sci. 377 (1997) 754-758, https://doi.org/S0039-6028(96)01488-4.

[51] L. Huang, L. Gan, N. Wang, X. Quan, B.E. Logan, G. Chen, Mineralization of pentachlorophenol with enhanced degradation and power generation from air

cathode microbial fuel cells, Biotechnol. Bioeng. 109 (2012) 2211-2221, https://doi.org/10.1002/bit.24489.
[52] L. Cao, W. Sun, Y. Zhang, S. Feng, J. Dong, Y. Zhang, B.E. Rittmann, Competition for electrons between reductive dechlorination and denitrification, Front. Environ. Sci. Eng. 11 (2017) 14, https://doi.org/10.1007/s11783-017-0959-x.
[53] F. Jiang, Y. Zhang, N. Sun, Z. Liu, Effect of direct current density on microstructure of tungsten coating electroplated from Na_2WO_4-WO_3-$NaPO_3$ system, Appl. Surface Sci. 317 (2014) 867-874, https://doi.org/10.1016/j.apsusc.2014.09.031.
[54] W. Li, H. Yu, Z. He, Towards sustainable wastewater treatment by using microbial fuel cell-centered technologies, Energy Environ. Sci. 7 (2014) 911-924, https://doi.org/10.1039/C3EE43106A.
[55] D. Jafarifar, M.R. Daryanavard, S. Sheibani, Ultra fast microwave-assisted leaching for recovery of platinum from spent catalyst, Hydrometallurgy 78 (2005) 166-171, https://doi.org/10.1016/j.hydromet.2005.02.006.
[56] H.L. Le, J. Jeong, J.C. Lee, B.D. Pandey, J.M. Yoo, T.H. Huyunh, Hydrometallurgical process for copper recovery from waste printed circuit boards (PCBs), Miner. Process. Extr. Metall. Rev. 32 (2011) 90-104, https://doi.org/10.1080/08827508.2010.530720.

Table 1 Separator factors in the 1# and the 2# units under various operational conditions

Fig. 1 Effect of various W concentrations on rates of (A) W and (B) Mo deposition, (D) current, and (E) cathode potential in the stacked BESs. (C) Applied voltage and (F) hydrogen production in the 1# unit of the stacked BESs. (initial Mo(VI) fixed at 1.0 mM, initial pH: 2.0, cathode: SSS in the 1# and CR in the 2# units).

Fig. 2 Effect of various Mo concentrations on rates of (A) W and (B) Mo deposition, (C) current, (D) cathode potential, (E) applied voltage, and (F) hydrogen production in the stacked BESs (initial W(VI) fixed at 1.0 mM, initial pH: 2.0, cathode: SSS in the 1# and CR in the 2# units).

Fig. 3 XPS analysis for (A, C, E and G) W and (B, D, F and H) Mo elements on the cathodes of (A, B, E and F) the 1# and (C, D, G and H) the 2# units at W/Mo molar ratios of (A, B, C and D) 1 : 0.01 or (E, F, G and H) 0.01 : 1 (initial pH: 2.0, cathode: SSS in the 1# and CR in the 2# units).

Fig. 4 EIS analysis at W/Mo molar ratios of (A) 1 : 1, 0.1 : 1, 0.05 : 1 and 0.01 : 1, and (B) 1: 0.01, 1 : 0.05, 1 : 0.1 and 1 : 1 as well as (C) single W or Mo (initial pH: 2.0, cathode: SSS in the 1# and CR in the 2# units).

Fig. 5 Effect of initial pHs on rates of (A) W and (B) Mo deposition, (C) current, (D) cathode potential, (E) applied voltage and (F) hydrogen production in the stacked BESs (W : Mo = 1 : 1; cathode: SSS in the 1# and CR in the 2# units).

Fig. 6 XPS analysis for (A, C, E and G) W and (B, D, F and H) Mo elements on the cathodes of (A, B, C and D) the 1# and (E, F, G and H) the 2# units at an initial pH of (A, B, E and F) 1.5 or (C, D, G and H) 4.0 (W : Mo = 1 : 1, cathode: SSS in the 1# and CR in the 2# units).

Fig. 7 Effect of cathode material on rates of (A) W and (B) Mo deposition, (C) current, (D) cathode potential and (E) applied voltage in the stacked BESs. (F) Rate of hydrogen production in the 1# unit of the stacked BESs (W : Mo = 1 : 1; initial pH: 2.0).

Fig. 8 Rates of (A) W and (B) Mo deposition, (C) current, (D) cathode potential, (E) applied voltage and (F) hydrogen production as a function of equal W/Mo molar ratio (CR in the 1# unit and SSS in the 2 units, initial pH: 2.0).